

C.P. No. 910

C.P. No. 910



LIBRARY
ROYAL AIRCRAFT ESTABLISHMENT
BEDFORD.

MINISTRY OF AVIATION

AERONAUTICAL RESEARCH COUNCIL

CURRENT PAPERS

Thermal Conductance Tests on Cabin Wall Insulation Assemblies for a Supersonic Transport Aircraft

by

Ian I. McNaughtan and P. A. Keene

LONDON: HER MAJESTY'S STATIONERY OFFICE

1967

PRICE 16s 0d NET

U.D.C. No. 536.24 : 629.13.013.1-1/2 : 629.137.1 : 533.6.011-5

C.F. No.910*

August 1964

THERMAL CONDUCTANCE TESTS ON CABIN WALL INSULATION
ASSEMBLIES FOR A SUPERSONIC TRANSPORT AIRCRAFT

by

Ian I. McNaughtan

and

P. A. Keene

SUMMARY

Thermal conductance tests have been made on a number of insulation assemblies for the cabin wall of a supersonic transport aircraft at outer skin temperatures in the range 90-120°C. In all cases the test specimens were assembled onto structure representing the fuselage wall. In addition tests were made on a representative fuselage to floor beam joint. The results of the tests are presented and discussed, and the problems of insulating hot cabin walls are outlined.

*Replaces R.A.E. Technical Note No. Mech.Eng.405 - A.R.C. 27497

CONTENTS

	<u>Page</u>
1 INTRODUCTION	5
2 TEST RIG	6
2.1 Description	6
2.2 Instrumentation	7
2.3 Test procedure	7
3 DESCRIPTION OF SPECIMENS	8
3.1 General fuselage specimens	8
3.2 Floor beam specimen	11
4 RESULTS	11
4.1 General	11
4.2 Temperature	12
4.3 Heat balance	12
5 DISCUSSION	16
5.1 Equivalent conductance	16
5.2 Heat leakage factor	17
5.3 Structure heat flows	18
5.4 Insulation joints	19
6 CONCLUSIONS	20
7 ACKNOWLEDGEMENT	20
SYMBOLS	21
REFERENCES	22
APPENDICES 1 AND 2	24 - 27
TABLES 1 TO 10	28 - 37
ILLUSTRATIONS - Figs.1 - 26	-
DETACHABLE ABSTRACT CARDS	-

APPENDICES

<u>Appendix</u>		<u>Page</u>
1	- Thermal characteristics of materials	24
2	- Derivation of theoretical conductance of primary insulation	25

TABLES

<u>Table</u>		
1	- Primary insulation heat flow rate and conductance	28
2	- Summary of results. B198.1 test panel	29
3	- B198.2 test panel	30
4	- B198.2 Mod test panel	31
5	- B198.3 test panel	32
6	- B198.4 (20' specimen) test panel	33
7	- B198.5 test panel	34
8	- B198.7 test panel	35
9	- B198.6 floor beam test panel	36
10	- Heat flow up frame members	37

ILLUSTRATIONS

	<u>Fig.</u>
Diagram of thermal conduction test rig	1
Thermal conduction test rig assembly details	2
Details of panel structure and location of thermocouple stations. Panel B198.1	3
Details of a typical Bristol 198 test panel after testing	4
Typical Bristol 198 test panel after testing	5
Typical Bristol 198 test panel	6

ILLUSTRATIONS (CONTD)

	<u>Fig.</u>
Details of attachment of insulation to structure. Panel B198.1	7
Details of attachment of insulation to structure. Panel B198.2	8
Details of attachment of insulation to structure. Panel B198.3	9
Details of attachment of insulation to structure. Panel B198.4	10
Details of attachment of insulation to structure. Panel B198.5	11
Details of attachment of insulation to structure. Panel B198.7	12
Diagram of floor beam attachment. Panel B198.6	13
Bristol 198 (floor beam) Panel 6	14
Details of modified floor beam panel	15
Details of construction and attachment. Panel B198.6	16
Typical temperature distribution. Panel B198.1	17
Typical temperature distribution. Panel B198.2M	18
Typical temperature distribution. Panel B198.3	19
Typical temperature distribution. Panel B198.4	20
Typical temperature distribution. Panel B198.5	21
Typical temperature distribution. Panel B198.7	22
Typical temperature distribution. Panel B198.6	23
Typical temperature distribution. Panel B198.6M	24
Comparison of heat input and calculated heat flow through primary insulation. Panel B198.4	25
Variation of structure heat flows with cooling air mass flow. Panel B198.6	26

1 INTRODUCTION

In order that an efficient cabin cooling system may be provided on a high speed aircraft, an accurate assessment must be made of the heat load on the system. One of the major heat loads is the heat that flows into the cabin as a result of aerodynamic heating of the skin during high speed flight. This heat load can be reduced by the application of thermal insulation to the cabin wall, but the weight of this insulation should then be included in the cooling system weight for assessments of overall design efficiency. In order to obtain the optimum distribution of weight between the insulation and the system and to assess the heat load on the system knowledge is required of the thermal resistance of the cabin wall insulation.

The cabin walls frequently have structural members extending from the hot aircraft skin into, or even through, the thermal insulation assembly. These members present little resistance to heat flow, compared with the insulation resistance, and it is difficult to calculate their effect on the thermal resistance of the composite structure and insulation assembly. A similar problem is encountered with the physical attachments of the insulation to the cabin wall structure. These factors make it impracticable to derive accurately the thermal conductance of a combined structure and insulation assembly from basic conductivity information, and recourse must be made to experiment or empirical formulae derived from experimental results.

In order to investigate the problems of thermal insulation of hot cabin walls a series of thermal conductivity tests was made on specimens representing the fuselage passenger cabin of a supersonic transport aircraft with an outer skin temperature in the range 90-120°C. The tests were made in conjunction with an investigation¹ using electrical analogue technique and thermal tests² with a 20' long x 12' diameter insulated cabin test specimen. All the conductivity test specimens were 3' x 3' in area and the insulation scheme was designed to include an integral cooling air passage. This type of wall insulation and cooling scheme was selected for the test programme as a result of a study³ which indicated that at skin temperatures above 100°C wall cooling was more efficient than bulk insulation from the aspects of overall system design and passenger comfort. Consideration was mainly confined to the primary insulation between the outer skin and the cooling air passage.

The investigation was planned to:

- (a) develop a good insulation assembly of low weight and small thickness, using a limited range of currently available insulants,
- (b) determine the thermal conductance of the assembly,
- (c) Investigate the effect of low thermal resistance paths within the insulation,
- (d) Investigate the effect of mounting and attachments,
- (e) determine that the temperatures of the various insular layers were acceptable from the aspect of material degradation.

A total of seven specimens was tested of which six represented general fuselage wall construction and one contained a floor beam to fuselage joint. In order to obtain a representative result it was decided that the test specimen must contain at least one fuselage frame pitch and a pitch of 22" was selected as typical for this dimension. To reduce end effects a test specimen at least 50% greater in size was desirable and a size of 3' x 3' was selected to allow the tests to be made in an existing test rig which was available for the work and required only slight modification to accommodate the wall cooling type of insulation scheme proposed. In order to ensure that specimen construction and assembly were typical of aircraft standards the specimens were designed and manufactured by Bristol Aircraft Ltd (now the Filton Division of British Aircraft Corporation (Operating) Ltd).

2 TEST RIG

2.1 Description

The tests were made in a 3' x 3' thermal conductivity test rig of guard ring type which had been developed for the purpose of testing homogeneous insulation materials. Basically this rig consists of an inner light alloy open topped box 3' x 3' in area and 9" deep, provided with adjustable brackets for support of a test specimen which forms a lid to the box. A 1.8 kW electrical heater element formed from 19 s.w.g. nickel wire mounted on a 3' x 3' compressed asbestos frame is mounted inside this inner box and is the main heater for the conductance tests. This heater is powered through an 8 amp variable voltage transformer from the laboratory A.C. mains either directly or through a stabilised voltage transformer. As shown in Fig.1, the inner box is mounted on 2" long compressed asbestos supports inside an outer metal box of similar design but 3'4" x 3'4" x 11" in size with the space between the two boxes filled with mineral wool insulation. On the outer sides and base of this outer box are mounted guard heaters formed from evenly spaced Pyrotenax heating cables. The heating cables round the four sides of the box form one electric circuit and the base heater forms a second, both circuits being powered via 8 amp variable voltage transformers directly from the laboratory A.C. mains. A total of 32 copper-constantan thermocouples are attached to the outer surface of the inner box sides and base and 32 to the inner surface of the outer box sides and base, in such a manner that when the two boxes are assembled the couples are in adjacent pairs across the gap.

As shown in Figs.1 and 2, this guard ring box, containing the inner box, the specimen and main heater, is mounted inside a compressed asbestos box 3'6" x 3'6" x 12" on 1" compressed asbestos spacers and with the intervening gap filled with mineral wool. This outer box prevents excessive heat loss from the guard heaters and reduces the injury hazard to personnel examining the specimen when the test rig is operated at high temperature.

An air supply for the wall cooling duct within the test specimen was obtained from an electric fan supplying a 6" dia plenum chamber at the duct entry through a flow control valve, a variable output electric heater and an orifice plate for flow measurement section. Both the air supply ducting and the plenum chamber were well lagged to prevent temperature variation in the inlet air. A similar lagged plenum chamber was connected to the specimen wall cooling duct exit but this chamber exhausted directly to atmosphere. A

radiation shield of aluminium foil was mounted above the test specimen to reduce heat transfer from the surface by radiation to the laboratory and a variable speed fan was mounted above the test specimen to give an air movement equivalent to that within an aircraft cabin (< 40 ft/min).

2.2 Instrumentation

2.2.1 Electrical power Input power to the main heater was measured on a Cambridge sub-standard multi range wattmeter. The power supplied to the guard box heaters was not recorded.

2.2.2 Airflow The mass airflow to the wall cooling duct was measured with a standard orifice plate with D and D/2 tapings leading to water manometers. The airflow above the test specimen was measured with a velometer and the fan adjusted to give a reading of 30-40 ft/min.

2.2.3 Temperature In general temperatures in the test rig and test specimen were measured by means of copper-constantan thermocouples connected through cyclic switch boxes to a Honeywell Brown continuous chart recorder Type Y153X62(PSD 12)-X-50V or an equivalent recorder. For the measurement of metal surface temperatures the thermocouple junctions were formed by flash welding the individual wires to the metal surface at a distance of $\frac{1}{8}$ " - $\frac{1}{4}$ " apart. On non metallic surfaces, the thermocouples were beaded and the bead cemented to the surface with a suitable adhesive. In all cases caution was exercised, especially in the case of thermocouples within the test specimen insulation, to ensure that the wire from the junction followed an isothermal path for some distance from the junction to reduce the possibility of false temperature readings due to heat conduction along the thermocouple wires.

The measurement of the temperature of the wall cooling air at inlet and outlet and the temperature change between the two caused considerable difficulty and no really satisfactory method was devised. The reason for the difficulty was that the air duct in the specimen was some 36" long by 1" deep and stray heat flow from the test rig was conducted into the plenum chamber-duct junction. Initially three thermocouples were located at equidistant positions in both inlet and outlet ducts and switched either to record mean inlet and outlet temperatures on the recorder or to form a closed thermocouple loop and record the temperature difference on a millivoltmeter of 0 - 1.5 mV range. Subsequent to the tests on panel 2 these thermocouples were supplemented with resistance thermometer screens formed from 0.030" diameter high- α nickel wire wound on rectangular frame formers of flexible fibre sheet. These screens were built into bridge networks and were calibrated under controlled conditions before installation. The indication of temperature rise from these resistance wire screens was assumed to be more accurate than the difference in thermocouple readings.

2.3 Test procedure

The specimen was fitted with thermocouples, installed into the conductivity test rig and the cooling air duct plenum chambers were assembled into position and lagged. After a check on all instrumentation the main and guard heaters were turned on and the specimen raised to the required temperature: at the same time the cooling air temperature and mass flow were

adjusted and the "cabin air" circulation fan energised. As the required specimen skin temperature was approached the main heater power was slowly reduced until quasi stability was obtained. During this setting up period the guard heater controls were constantly adjusted to maintain thermal equilibrium between the inner and outer test rig boxes. The heater supply was then selected from the stabilised voltage supply and final adjustments made to the cooling air controls and guard system. After a settling period of one hour during which time a check was made that stability of temperature in the specimen was within acceptable limits, the instrument records were taken over a further period of at least one hour at 15 minute intervals.

After considerable trouble in obtaining stability it was found that the simplest procedure was to carry out the setting up procedure during the afternoon and allow the specimen to settle down under constant conditions overnight. The next morning minor corrections could be made and the required degree of stability of less than 2° /hour skin temperature change, could then be obtained and the test run completed during the morning. In the afternoon new conditions, such as a change in cooling air mass flow or temperature, could be selected, the heater controls adjusted and the specimen restabilised ready to settle in overnight for a test run the next morning.

Due to the high ratio of rig-specimen thermal capacity to main heater power the control was sluggish and any attempt to get quick results ended in failure. Although the method of test used was slow, in that it took about 3 weeks to test a specimen, it was found by experience to be the only acceptable method.

3 DESCRIPTION OF SPECIMENS

3.1 General fuselage specimens

3.1.1 Panel structure The majority of the specimens representative of the general fuselage insulation were assembled onto metal structures representative of the proposed construction in the forward fuselage of the Bristol 198 transport aircraft. The panel structure comprised a light alloy sheet $3' \times 3' \times 16$ s.w.g. representing the aircraft skin to which were attached Z-section stringers, $\frac{3}{4}" \times \frac{5}{8}" \times 18$ s.w.g., at 6" pitch and composite channel sections representing the fuselage main frames and subsidiary frames or crack stoppers, slotted to take the continuous stringers. There was no physical contact between the stringers and the frame members. As illustrated in Figs. 3-7 the 3" frames representing the main structure frames were constructed from a $2\frac{1}{4}" \times \frac{5}{8}" \times 20$ s.w.g. channel attached to a $1\frac{5}{8}" \times \frac{5}{8}" \times 20$ s.w.g. angle section which was attached to the panel skin. The 2" frame was constructed in a similar manner but the channel section was reduced to $1\frac{1}{4}" \times \frac{5}{8}" \times 20$ s.w.g. The panel structure had one main frame and one subsidiary frame mounted symmetrically on either side of the specimen centre line at a pitch of 11" (Fig. 3) and additional main frames near the panel edges at a distance of 11" from the central frames. The effect of this difference between panel and aircraft layout is discussed in para 5.2.

The structure used for panel B198.4 differed slightly in construction in that the composite frame construction was replaced by Z-section frame construction (this panel was representative of the construction used in the 20' long cabin test² specimen). In addition the stringers were 1.15" in height

as opposed to $\frac{3}{4}$ ". Panel B198.5 represented the aircraft rear fuselage and had composite frames 1" deeper than those in panels B198.1 to 4. The main frames were 4" deep and the subsidiary frame 3" deep. The stringer height was 1.15" as in panel B198.1. Material thicknesses and frame stringer pitch were unaltered.

All joints in the structure were conventional riveted joints and all the "internal" metal surfaces were treated with corrosion resistant paint after assembly. The frames and stringers did not extend fully across the panel but were stopped off $\frac{1}{2}$ " from the panel edges to allow assembly of a Durestos box structure around the panel as shown in Fig.3. This box acted as an attachment for the edges of the thermal insulation layers and prevented circulation of hot air from the test rig heater into the specimen.

3.1.2 Thermal insulation The thermal insulation on all six test panels representing the general fuselage insulation assembly was of wall cooling type. In conformity with general usage the portion of insulation between the specimen skin (i.e. outer aircraft skin) and the integral cooling air duct is referred to as the Primary Insulation, and the Secondary Insulation refers to the insulation between the air duct and the cabin interior. Details of the insulation assemblies and the methods of attachment to the structure are given in Figs.7 to 12.

In all cases the edges of the rigid primary insulation layer were attached to the Durestos box structure. At the entry and exit of the integral wall cooling air passage in the insulation, formed glass cloth/plastic laminate connector pieces were fitted to duct the cooling air from and to the air plenum chambers. The side walls of the air passage were formed from channel sections, of appropriate depth, secured to the joint between the Durestos box and the primary insulation. The side edges of the secondary insulation layer were attached to these channels and also to the duct entry and exit connector pieces.

In addition to edge mounting of the insulation assemblies an attachment was provided to secure the insulation assembly to one of the panel frame members. This frame attachment represented the aircraft mounting and was designed to give adequate strength of attachment of the insulation layers to the structure and also to allow removal and re-attachment of the various insulant layers. This latter feature was required in the test specimens to allow installation of temperature measuring devices and would be required on an aircraft installation for inspection purposes.

Panel B198.1 This insulation assembly, Fig.7, was selected as an initial test specimen to act as a datum typical of current practice thermal insulation modified to wall cooling type. The primary insulation consisted of a 2.85" Microlite glass fibre blanket faced on its outer (hot) surface with 0.0007" aluminium foil and cemented to a 0.014" thick laminated plastic sheet. This laminate acted as a structural support for the primary insulation and as the outer wall of the cooling air duct. The glass fibre blanket was cut away to accommodate the panel frame members. The primary insulation was attached to the 2" subsidiary frame by light alloy bolts secured by speed nuts to Durestos brackets spaced at 6" pitch and a plastic spacing strip was inserted above the 3" frame member flange to prevent it

contacting the primary insulation. The cooling air passage was 1" deep and this value was maintained by a number of spacer columns in addition to the edge channels and mounting attachment Z-section member. The secondary insulation consisted of $\frac{5}{8}$ " Plasticell type D40 sheet. Details of the insulation material properties are given in Appendix 1.

Panel B198.2 was similar in attachment and secondary insulation to panel B198.1 but the primary insulation was modified by replacing the laminate with Plasticell type D40 sheet of $\frac{5}{8}$ " thickness and reducing the Microlite glass fibre blanket thickness to 2". An overall depth of 3.85" was retained between the metal panel outer skin and the air duct wall by increasing the air gap between the metal panel and the aluminium foil layer. These modifications increased the stiffness of the primary insulation layer and the plastic spacers required in panel B198.1 were deleted.

As shown in Fig.8, this specimen was subsequently modified, to panel B198.2M, by the addition of strips of $\frac{5}{8}$ " Plasticell type D40 in the integral air duct above the frame members.

This modification was made in an attempt to reduce the heat flow up the frames.

Panel B198.3 The bulk insulation layers of this panel were identical with those of Panel B198.2 but the mounting method differed in that attachment of the primary insulation to the panel structure was transferred from the 2" secondary frame to the 3" main frame and the air duct depth was increased from 1" to $1\frac{1}{8}$ ". The additional Plasticell strip in the air gap above the main frame, as developed in panel B198.2M, was retained and the strip above the subsidiary frame was transferred to a position between the frame flange and the $\frac{5}{8}$ " Plasticell sheet as shown in Fig.9.

Panel B198.4 In this panel the bulk primary insulation was again the same as panels B198.2 and .3 but the method of attachment to the main frame members was considerably developed to be more representative of an aircraft installation. The secondary insulation was reduced to a $\frac{1}{4}$ " layer of plastic sponge backed with a thin glass cloth laminate to provide rigidity. Details are given in Fig.10.

Panel B198.5 was of similar design in mounting details to panel 3 but the thickness of the glass fibre blanket was increased from 2" to 3" to accommodate the increased depth of frame members and Fibreglass material was used in place of Microlite. The air passage depth was reduced to 1", as shown in Fig.11.

Panel B198.7 Fig.12, had a primary insulation assembly formed from moulded Plasticell type D45/50 sheet with a layer of aluminised Melanex cemented to the outer surface (facing the hot structure assembly). The secondary insulation layer was identical with that used on panel B198.4. The assembly attachment to the 3" frame was of similar design to that used on panel B198.4.

3.2 Floor beam specimen

3.2.1 This test specimen, panel B198.6, was representative of the joint between the fuselage wall and a passenger cabin floor beam. It was tested to investigate the problems associated with such major structural assemblies penetrating through both the insulation assembly and the integral air passage. Fig.13 shows diagrammatically the region represented by the test panel and indicates how the floor beam acts as a low thermal resistance path for heat to flow from the hot aircraft skin through the insulation assembly into the passenger cabin and under-floor compartment in addition to possible heat flow into the cooling air passage itself.

3.2.2 Details of panel structure Figs.14 and 15 shows structural details of the panel with the insulation removed but with the Durestos edge box in position. Additional details are given in Fig.16. The panel was a 3' x 3' x 16 s.w.g. light alloy plate with Z-section stringers 1.15" x $\frac{5}{8}$ " x 18 s.w.g. as in specimen panel B198.5. The specimen carried a central main frame 4" deep with a 3" subsidiary frame either side, the frames being identical with those in panel B198.5. Also attached to the skin were two 4" deep longerons of Z-section formed from 18 s.w.g. light alloy. The frames, and stringers were riveted to the simulated skin and the floor beam longerons were attached to the skin by bolts. The floor beam was a composite channel formed from an 18 s.w.g. light alloy plate reinforced along its edges with angle section to form a 4" x 1" channel. It was attached to the 4" frame member and to the two Z-section longerons by means of angle sections secured by bolts. As indicated in Fig.15, provision was made in the design for the introduction of Durestos packing pieces into all the bolted joints to allow testing both with and without joint packing. It can also be seen in Fig.15 that the stringers were cleated to the frame members, a feature which was not introduced on any of the other specimens.

The floor beam was reduced to 18" in length, for convenience in handling the specimen, and had a representative area of floor (including a seat rail), under-floor skin and box structure attached as shown in Figs.14 and 16. This structure was secured to the beam by means of bolted joints with provision for Durestos packing pieces between the metal faces.

3.2.3 Details of insulation The primary insulation was identical with that applied to panel B198.5 except where modified to take the floor beam (Fig.16). The main modification was that a Durestos air passage moulding was fitted over the floor beam, and connected to mountings on the floor beam longerons. This Durestos structure shielded the floor beam from the air in the cooling air passage and acted as an attachment for both the primary and secondary insulation layers. The secondary insulation was a composite glass cloth laminate/foam plastic layer as used in panel B198.4 with the addition of a layer of Royalite cabin trim material. The joints in this innermost layer were covered with a coping strip as in panel B198.4.

4 RESULTS

4.1 General

In general the tests were made at nominal skin temperatures of 100°C and 120°C, a range of cooling air inlet temperature of 20°C to 30°C and mass

flows of 4, 6, and 8 lb per minute per specimen. This mass flow rate is equivalent to 1.33, 2 and 2.66 lb/min per foot of panel specimen length.

4.2 Temperature

Typical temperature distributions within the various specimens are given in Figs. 17 to 24.

4.3 Heat balance

4.3.1 Heat flow One of the objects of the experiments was to determine and compare the thermal resistances of the various insulation assemblies. Since the specimens were of wall cooling type and since only two secondary insulation assemblies were tested it is more convenient to compare the conductances of the various primary insulation assemblies based on the temperature difference between metal skin surface and air passage mean air temperature. However, as described in para 3.1.1, the ratio of main frame members to subsidiary frame members in the test panel structure differed from the ratio proposed for the projected aircraft and since the heat flows in these frame members were different, and of significant magnitude compared to the heat flow in the bulk insulation, the total heat flow through the specimen would not be the same as the heat flow through a similar area of aircraft fuselage. To obtain the equivalent conductance of the primary insulation - that is the conductance applicable to the aircraft fuselage based on an area of surface containing the correct proportion of main frame subsidiary frame and bulk insulation - it was necessary to determine in each case the heat flow in both main and subsidiary frames and in the bulk insulation remote from the frames, and to sum these values in a particular manner as discussed in para 5.1 below. In all the tests adequate experimental measurements were made to allow these heat flows to be derived and the values obtained were used to calculate the total heat flow through the primary insulation layer of the specimen (q_T).

Under ideal conditions of balanced guards and stability of temperature this heat flow through the primary insulation (q_T) should equal the heat input from the main heater (q_{IN}) and also the heat output from the specimen (q_{OUT}) which is the sum of the heat gained by the cooling air plus the heat flow through the secondary insulation. If this equality was obtained it could be assumed that the experimentally derived values of heat flow up the frame members and through the bulk primary insulation were correct and an equivalent conductance for the aircraft case could be reliably calculated. Under the conditions of test this equality was not obtained and the accuracy of the various methods must therefore be examined to determine if the experimentally derived values of frame and insulation heat flow are acceptably accurate.

4.3.2 Primary insulation heat flow The heat flow through the primary insulation was obtained by summing the frame member heat flows and a proportion of the bulk primary insulation heat flow remote from the frames. The heat flow up the frame members (q_F/c) per unit length of frame was derived from

$$q_F/c = k_F A_F \Delta T_F / d_F \quad \text{CHU/ft hr} \quad (1)$$

where k_F = theoretical conductivity of the material CHU/ft² hr^oC/ft
 A_F = area per unit length of frame = ft²/ft
 ΔT_F = measured temperature gradient in ^oC in the frame over a distance of d_F feet in the direction of heat flow.

In the tests $\Delta T_F/d_F$ was the mean of at least two sets of values for both main (q_F/l) and subsidiary (q_s/l) frame heat flows. The heat flow in the bulk primary insulation remote from the frames (q_P/A) was derived from

$$q_P/A = \frac{\Delta T_P}{R_P} \text{ CHU/ft}^2 \text{ hr} \quad (2)$$

where R_P = thermal resistance of the bulk assembly ft² hr^oC/CHU
 $= \sum \frac{d}{k}$

where k and d are the theoretical conductivities and actual dimensions of the composite assembly,

and ΔT_P = recorded temperature gradient over the thickness $(\sum d)$ of the composite assembly.

In an area of insulated structure containing frame members the total heat flow (q_T) can be expressed as the total frame member heat flow ($q_{F1} + q_{F2} \dots$) plus a fraction F' of the bulk insulation heat flow (q_P) i.e.

$$q_T = (q_{F1} + q_{F2} \dots) + F' q_P$$

The value of F' depends on parameters such as insulation thickness, frame size, frame pitch, insulation conductance etc and varies from unity, when no frames are present, to zero when the whole heat flow passes up the frames. From tests with an electrical analogue¹ the value of this factor was determined for panel B198.3 and gave the relationship

$$q_T = 3 \times 3 \times q_F/l + 3 \times q_s/l + 9 \times 0.83 \times q_P/A \text{ CHU/hr} \quad (3)$$

for a specimen 3' x 3' = 9 ft² in area containing 3 main frame members 3' in length and one subsidiary frame 3' in length. This relationship was also used for panels B198.1, B198.2, B198.4 and B198.7.

In the case of panel B198.5 analogue tests provided the relationship

$$q_T = 9 q_F/l + 3 q_s/l + 9 \times 0.68 q_P/A \text{ CHU/hr} \quad (4)$$

Using equations (3) or (4) as appropriate, the value of the heat flow through the primary insulation assembly was derived.

4.3.3 Heat input The heat input to the specimen (q_{IN}) was obtained by recording the power supplied to the main rig heater by means of an accurate wattmeter. Since absolute stability of temperature within the test specimen could not be maintained this steady input power was supplemented by the heat absorbed or released by the specimen corresponding to the temperature change. This supplement was of the order of $\pm 5\%$ of the steady input power and was calculated from

$$S = \sum (M C_p dT/dt) \text{ CHU/hr} \quad (5)$$

where S = heat supplement CHU/hr

M = component mass lb

C_p = component specific heat CHU/lb $^{\circ}$ C

dT/dt = mean rate of change of temperature $^{\circ}$ C/hr.

4.3.4 Heat output The heat output from the specimen (q_{OUT}) was the sum of the heat gained by the cooling air (q_A) plus the heat flow through the secondary insulation (q_S). These values were calculated from

$$q_A = \dot{M}_A C_{pA} \Delta T_A \times 60 \text{ CHU/hr} \quad (6)$$

where \dot{M}_A = cooling air mass flow in lb/min

C_{pA} = specific heat of air

ΔT_A = recorded temperature gradient from inlet to outlet from the integral air passage

and

$$q_S = \frac{A_S \Delta T_S}{R_S} \text{ CHU/hr} \quad (7)$$

where ΔT_S = recorded temperature gradient across the secondary insulation layer in $^{\circ}$ C

R_S = thermal resistance of the secondary insulation assembly
ft 2 hr $^{\circ}$ C/CHU

A_S = surface area of the secondary insulation = 9 ft 2 .

4.3.5 Heat balance The values of q_T , q_{IN} and q_{OUT} derived from the various tests are given in Tables 2 - 9 and it can be seen that specimen heat balance, indicated by equality of these heat flows, was not obtained.

It is considered that the value of q_{IN} is an accurate measure of the heat input but close examination of the specimen/test rig assembly reveals that it is unlikely that q_{IN} is an accurate measure of the heat flow through the specimen, for the following reasons.

(1) The presence of the frame members within the insulation result in a far from homogeneous assembly and an irregular temperature distribution must be obtained at the specimen sides containing the frame member ends. The side guard heaters were not graded to conform to this irregular distribution so that it is considered that, even with guard heaters adjusted to indicate mean equilibrium temperature, there would be some heat flow outwards through the guards at these side positions.

(2) There was no guard along the top edge of the inner box sides and this 12' of edge would allow heat loss from the main heater.

On this basis the value of q_{IN} should be greater than q_T and the discrepancy should increase with temperature. Fig.25 shows a plot of q_{IN} and q_T for panel B198.4. The plot shows a value of $(q_{IN} - q_T)$ increasing with increase in heat flow (i.e. with temperature) and an average value of the difference in the order of some 20 watts. This is the order of discrepancy that would be expected. Similar results can be obtained from the results from the other test specimens.

It is therefore considered that, although the values of q_T and q_{IN} are not equal, there is no indication that q_T are incorrect but rather that they are probably sufficiently accurate for comparative purposes.

With regard to heat output from the specimen, q_{OUT} , great difficulty was experienced in the accurate measurement of the temperature rise of the cooling air during its passage through the specimen. This temperature rise varied, theoretically, over the range 0.5 to 2°C so that a $\frac{1}{2}$ °C error in measurement is equal to a 100% - 25% error in estimate of heat gain by the air. The problem was further increased by the elongated shape of the air duct, 36" x 1" in cross section and by the complicated heat flow within it. As stated in para 2.2.3 the method of measurement of this temperature difference was developed during the test programme but it is considered that the accuracy finally attained was not of a high enough order to allow comparison with the derived values of heat flow through the primary insulation layers.

Since the derived primary insulation heat flow is in agreement with the power input, allowing for heat losses, and since the derived values of heat output are suspect it is considered that comparison of equivalent conductance values for the various insulation assemblies based on the derived primary insulation heat flow is acceptable.

Values of equivalent conductance and heat flow for the primary insulation layers are given in Table 1.

4.4 Floor beam joint

In the case of the floor beam joint specimen no attempt was made to derive q_m in view of the complication of the specimen. The main heat flow results are presented separately in Fig. 26. Two cases are given. The modification which was made to the specimen consisted of the insertion of Durestos packing pieces into the joints between the skin and the floor beam longerons, between the longerons and the frames and in the floor beam assembly.

5 DISCUSSION OF RESULTS

5.1 Equivalent conductance

As discussed in paras 3.1.1 and 4.3.1 the difference in frame distribution between the test specimens and the aircraft case requires that the primary insulation conductance in the aircraft case be calculated from the specimen individual heat flows and cannot be obtained directly from the specimen total heat flow. It is only on the basis of the aircraft installation that the various assemblies can be compared. An equivalent square foot of aircraft fuselage would be an area one main frame pitch in width containing a subsidiary frame and the appropriate area of bulk insulation attachments and internal ducting. In the case of the B198 project the frame pitch is 22 inches and the equivalent area is therefore 22 inches in width and $144/22 = 6.55$ inches or 0.545 feet in length: the frame members would be 0.545 feet long. Using the electrical analogue values quoted in para 4.3.2 for the modifying effect of frame members on heat flow through the bulk insulation the equivalent conductance k'/l based on the temperature difference between simulated skin and air passage mean air temperature can be expressed as

$$k'/l = \left[0.545 \left(q_P/l + q_C/l \right) + 0.83 q_P/A \right] / \Delta T \quad \text{CHU/ft}^2\text{hr}^\circ\text{C} \quad (8)$$

and

$$k'/l = \left[0.545 \left(q_P/l + q_C/l \right) + 0.68 q_P/A \right] / \Delta T \quad \text{CHU/ft}^2\text{hr}^\circ\text{C} \quad (9)$$

for the specimens with 3" and 4" main frame members respectively,

where q_P/l = measured heat flow per ft length up main frames in CHU/ft hr

q_C/l = measured heat flow per ft length up subsidiary frames in CHU/ft hr

q_P/A = measured heat flow₂ per ft² through bulk primary insulation remote from frames CHU/ft² hr

ΔT = temperature difference between outer skin and mean air passage temperature °C.

The values of equivalent conductance for the fuselage insulation specimens are given in Table 1. The value of k'/ℓ for specimen B198.1 was $0.146 \text{ CHU/ft}^2 \text{ hr}^\circ\text{C}$. The difference in construction between panels B198.1 and B198.2 was mainly the replacement of 0.85" of glass fibre blanket by $\frac{5}{8}$ " of foamed plastic insulant. This made no significant difference to the conductivity value derived. When specimen B198.2 was modified in an attempt to decrease the frame heat flows the value of k'/ℓ was reduced to 0.139. In tests of specimen B198.3, basically similar to B198.2 except that the attachment was changed from the subsidiary frame to the main frame, the conductance was found to vary from $0.143 \text{ CHU/ft}^2 \text{ hr}^\circ\text{C}$ at a cooling air flow of 1.33 lb/ft min to $0.179 \text{ CHU/ft}^2 \text{ hr}^\circ\text{C}$ at a flow of 2.67 lb/ft min. This rise in k'/ℓ is attributed to cooling air leakage from the cooling air duct into the zone below the primary insulation at the joint attachment which was found to be slightly distorted after test. The rise in conductance of 25% would be serious if it occurred in the aircraft and indicates the need for good integrity of insulation attachment joints. Panel specimen B198.5 followed B198.3 in chronological sequence and is basically the same design adopted for 4" frame members in place of 3" ones. Care was exercised in sealing the attachment joints to prevent air circulation. A conductance of $0.102 \text{ CHU/ft}^2 \text{ hr}^\circ\text{C}$ was obtained which compares well with that from specimen B198.3 at low airflow when allowance is made for the increased thickness of bulk insulation.

Test specimen B198.4 was designed to prevent air leakage at the air passage attachment joint to the main frame and the joint assembly was more representative of aircraft standards. The resulting value of conductance of $0.120 \text{ CHU/ft}^2 \text{ hr}^\circ\text{C}$ was the lowest achieved of the test panels with 3" frame members and the assembly was used in the 20' long cabin test specimen. In the tests² of this cabin specimen a similar primary insulation conductance was recorded thus justifying the conclusions of para 4.3.5.

Specimen B198.7 was tested to investigate the use of more rigid assemblies but the high value of $k'/\ell = 0.245$ was obtained. This value was higher than was anticipated and examination of the specimen after test showed that the foam plastic layer had distorted between the frame members and had come into direct contact with the panel stringers and the subsidiary frame thus reducing the thermal resistance of the air gaps and increasing the overall heat flow.

5.2 Heat leakage factor

If the equivalent conductance, k'/ℓ , of the primary insulation (or of the total insulation assembly if wall cooling is not employed) is compared with the theoretical conductance $(k/\ell)P_{th}$, of the insulation remote from the frame the difference in value can be attributed to the effect of the relatively low thermal resistance paths of the frame members and attachment fittings. The ratio $(k'/\ell)/(k/\ell)P_{th}$ is generally referred to as the heat leakage factor. In the assessment of cooling system loads in project studies the value of $(k/\ell)P_{th}$ can be calculated for a proposed insulation assembly and a value of heat leakage factor applied to allow calculation of the heat load. Values up to 2.0 have been suggested¹ for this factor.

The theoretical conductance of the primary insulation assemblies are given in Table 1. These values include the thermal resistance of the air gap between the skin and the primary insulation and were calculated in the manner described

in Appendix 2 for specimen B198.4. The resultant heat leakage factors are also given in Table 1 and can be seen to lie in the range 1.25 to 1.5 except for values of 1.69 and 1.82 obtained in tests of specimen B198.3 where the high value is attributed to joint breakdown.

It is considered that for structural make up of the type tested (conventional dimensions for a large passenger transport fuselage) the value of 2.0 for the heat leakage factor is high and would represent a poor thermal design. Reasonable care in the design of joints and attachments should allow a factor of 1.5 to be achieved and extreme care and attention to detail could reduce this to 1.25. This of course only applies to the bulk fuselage. The presence of windows, doors, floor beams etc must be allowed for additionally.

5.3 Structure heat flows

5.3.1 Frame member heat flow In discussing the heat flow into the primary insulation along the low thermal resistance paths offered by the frame members, it is convenient to consider the results in terms of the aircraft case. In Table 10 the results are presented on the basis of an equivalent square foot of fuselage with the outer skin at 120°C and a mean cooling air temperature of 20°C.

There is little difference between the results of specimens 1 and 2, some 44% of the heat flow was equally divided between the main and subsidiary (attachment) frames. The insulation added to specimen 2M above the frame members reduced the frame heat flows by some 15%.

In the case of specimen 3, and subsequent specimens, the insulation attachment to the structure was removed from the subsidiary frames to the main frames. Although this had little effect on the overall result, the subsidiary frame heat flow reduced from 2.63 to 1.59 CHU/hr and the main frame flow increased from 2.77 to 4.07 CHU/hr indicating the effect of heat flow through attachments. Also indicated in the results from specimen 3 was the large increase in heat flow which could result from faulty attachment design. Due to material distortion at the attachment joint on the main frame some circulation of air between the air duct and the airspace around the frame was allowed with corresponding transport of heat into the air duct. This is reflected in the 3" frame heat flow and the total heat flow per square foot which increased from 14.3 to 17.9 CHU/hr, an increase of 25%, for a cooling air flow increase of 1.33 lb/min ft to 2.67 lb/min ft. In general the effect on heat flow of increase in airflow was too small to be separated from experimental scatter in results.

Specimen 4 incorporated the best engineered attachment joint and this is reflected in the low values of frame heat flow and overall heat flow which were obtained under test. Nevertheless nearly 30% of the heat flowed up the frame members.

The results from specimens 5 and 6 (floor beam specimen) are comparable in so far as the frame members are the same size. It can be seen that in the case of specimen 6 the frame heat flows were affected by leakage and widely different results were obtained between the modified and unmodified specimens although the modification itself in no way altered the thermal resistance of the frame member heat flow paths. The removal and re-attachment of the insulation

would appear to have increased the leakage effect and increased the frame heat flows. The minimum values for the tests on specimen 6 are comparable with those on specimen 5.

5.3.2 Stringer heat flow Heat flow up the stringer webs was measured in some tests by determining the temperature gradient $\Delta T/l$ up the web. This temperature gradient was of the order of 0.3°/in. and therefore indicates that the stringers are acting as fins assisting heat flow from the skin to the primary insulation. An increase of 10% in conventional heat transfer area was made to allow for stringer fin effect in deriving the theoretical conductance of the bulk primary insulation as described in Appendix 2.

5.3.3 Floor beam heat flow The heat flow up the floor beam, measured by determining the temperature gradient in the beam, is presented in Fig.26 in CHU/hr°C based on the difference between the simulated skin and cabin air temperatures and is the heat flow from one floor beam joint. These results suggest that the majority of the floor beam heat passed directly into the simulated internal cabin structure - i.e. floor, seat rails etc. For the case of a skin temperature of 120°C and a cabin/under floor temperature of 20°C each floor beam would contribute some 50 CHU/hr (25 watts) to the cooling system load by virtue of the beam/fuselage joint. An additional heat flow, in this case to the wall cooling air, results through the floor beam longerons. As shown in Fig.26 this heat flow is similar, in order, to that in the main frame members and in the specimen tested it appeared to be subject to variation due to air leakage at attachment joints.

5.3.4 Packing pieces The effect of thermal insulation packing pieces in metal joints of the floor beam and in the floor beam and longeron to fuselage joints was negligible. The thermal resistance of the packing pieces is small and adequate convective heat transfer around the joints negates any effect they have. As shown in Fig.26, the effect of the packing pieces was completely masked by changes in attachment joint leakage.

5.4 Insulation joints

The thermal insulation applied to aircraft cabin walls is generally required to be removable to allow periodic inspection of the structure. This requires that the installation is applied to the structure in segments or panels, each segment being joined to the adjacent ones. The test specimens included typical joints of this type. The structure heat flows in specimens 3 and 6 indicated the changes in thermal resistance which can result if the joints are not carefully designed. Although the specimen joints were readily accessible for inspection considerable decrease in thermal resistance resulted after the joint was broken and reassembled. On an actual aircraft installation there would be many joints and some would be in positions where both assembly and inspection would be difficult. Unless the joints were designed on an engineering basis with a view to reassembly, it is most probable that the initial thermal resistance would not be achieved after the first and subsequent reassemblies, with a consequent deterioration in comfort for the cabin occupants.

6 CONCLUSIONS

6.1 A satisfactory thermal insulation assembly of wall cooling type was developed using conventional materials (glass fibre blanket and foamed plastic sheet) which was considered adequately representative of current aircraft practice for use in full scale heat flow experiments with a cabin specimen 12 ft in diameter and 20 ft in length. The temperatures measured during the tests indicated that the materials were working within acceptable limits.

The thermal conductance of the primary insulation of this assembly was determined as $0.12 \text{ CHU/ft}^2 \text{ hr}^\circ\text{C}$ based on the temperature difference between the outer skin and the air in the wall cooling duct [Specimen B198.4].

6.2 The adverse affect on thermal resistance of low resistance heat flow paths within the insulation assembly was clearly demonstrated. In the estimation of passenger cabin heat loads due allowance must be made for the effect of fuselage structure within the thermal insulation. In the case of aircraft of generally similar structural make up to the specimens tested and described in this note it is recommended that the theoretical heat flow through the bulk fuselage thermal insulation should be factored by 1.5 to allow for this affect. If extreme care is taken in the design of the joints in the insulation layers and in the methods of attachment this factor may be reduced to a value not less than 1.25.

It is emphasised that this factor of 1.5 makes no allowance for the effects of windows, floor beams, bulkheads, doors etc which will provide added heat flows. The order of heat flow at floor beam joints to the fuselage can be obtained from the results of the tests on specimen B198.6.

6.3 In the design of fuselage thermal insulation assemblies for aircraft with hot outer skins attention must be paid to the effect of the low thermal resistance heat paths of attachments and to the integrity of joints. These problems are aggravated by the need to remove the insulation periodically to allow inspection of the fuselage well.

Direct low thermal resistance paths, such as attachment screws, should not be provided from the hot structure to any cooling air flow or directly into the passenger compartment.

Joints in the insulation layers should be designed to prevent any passage of hot air from the outer air gaps to the cooling air passages or cabin interior. In the design of these joints due consideration must be given to the effect of distortion caused by pressure changes, thermal expansion or thermal degradation of the materials used.

7 ACKNOWLEDGEMENT

Acknowledgement is made of the assistance of British Aircraft Corporation (Operating) Ltd, Filton Division, in the design and construction of the various test specimens and of their co-operation in the performance of the tests and analysis of the test results.

SYMBOLS

A	= area	ft ²
C _p	= specific heat	CHU lb ⁻¹ °C ⁻¹
D	= diameter	ft
d	= distance	ft
F'	= non-dimensional factor	
h	= heat transfer coefficient	CHU ft ⁻² hr ⁻¹ °C ⁻¹
k	= thermal conductivity	CHU ft ⁻¹ hr ⁻¹ °C ⁻¹
k'/ℓ	= equivalent conductance	CHU ft ⁻² hr ⁻¹ °C ⁻¹
	= thermal conductance of a representative square foot area of aircraft surface	
L	= length	ft
ℓ	= length	ft
M	= mass	lb
N _{RA}	= Rayleigh Number	
Q	= heat quantity	CHU
q	= heat flow	CHU hr ⁻¹
R	= thermal resistance	ft ² hr °C CHU ⁻¹
S	= heat supplement	CHU/hr
T	= temperature	°C or °K
t	= time	hours
x	= distance	ft
ΔT	= temperature difference	°C
ε	= emissivity	
σ	= Stephans Constant	CHU ft ⁻² hr ⁻¹ °K ⁻⁴

SYMBOLS (CONTD)

Suffices

A = air
AL = aluminium foil
C = subsidiary frame member
C' = convective
F = main frame member
f = film
IN = input
OUT = output
P = primary insulation assembly
P_{th} = primary insulation assembly theoretical value
r = radiative
S = secondary insulation assembly
S' = skin
S'' = stringer
T = total

REFERENCES

<u>No.</u>	<u>Author</u>	<u>Title, etc.</u>
1	McNaughtan, I.I. Hughes, T.L. Fielding, D.	A study of the thermal properties of aircraft cabin insulation using electrical analogue technique. A.R.C. 24047, April 1962
2	Hughes, T.L. Timby, E.A.	Air distribution tests on a supersonic transport aircraft cabin. R.A.E. Technical Report 66118
3	Timby E.A.	Cabin wall cooling systems for very high speed flight vehicles. A.R.C. 26084, March 1964
4	McAdam, H.W.	Heat transmission. 3rd edition, McGraw Hill 1954

APPENDIX 1

THERMAL CHARACTERISTICS OF MATERIALS

1 In the calculation of heat flows within the insulation and structure of the test panels the values of the various parameters used are given below.

2 Glass fibre blanket

Thermal conductivity.

"LOF Microlite" glass fibre as shown in Fig.1.

"Fibreglass" glass fibre as shown in Fig.2.

Density 0.60 lb/ft³.

Specific heat 0.20 CHU/lb^oC.

3 Plasticell sheet

Thermal conductivity.

Type D 40/45. $0.20 + 0.002T$ CHU/ft² hr^oC/in. for T in ^oC.

Type D 45/50. $0.15 + 0.002T$ CHU/ft² hr^oC/in. for T in ^oC.

Density 3.0 lb/ft³.

Specific heat 0.25 CHU/lb^oC.

4 Light alloy

Thermal conductivity 1200 CHU/ft²hr^oC/in.

Density 169 lb/ft³.

Specific heat 0.21 CHU/lb^oC.

APPENDIX 2

DERIVATION OF THEORETICAL CONDUCTANCE OF THE PRIMARY INSULATION

1 Considering the bulk primary insulation assembly remote from frame effects, the heat flow through the primary insulation (q_p/A) is equal to the heat transferred across the air gap from the hot skin to the aluminium foil surface. This latter heat flow is a combination of radiative, convective and conductive heat flow and is largely a function of T_S , the hot skin temperature, and T_{AL} , the aluminium foil temperature. The heat flow through the primary insulation is a function of the temperatures of the individual layers, since the materials used have conductivities which are temperature dependent, and can be considered as a function of T_{AL} and T_A , the cooling air temperature, and the cooling air velocity. Since the heat flow, and hence the conductivity, is a function of a number of variables its calculation presents some difficulty. However a close approximation to its value was obtained in the following manner.

2 The skin temperature, T_S , was assumed to be 120°C [393°K] and the heat flow from the skin to the aluminium foil was calculated, as described below, for various values of T_{AL} .

The air temperature T_A was assumed to be 20°C and the mass flow 2 lb/min ft width of duct. Using these values the heat flow from the aluminium foil was calculated for various values of T_{AL} and using conductivities appropriate to the temperature distribution in the insulation layer.

The two resulting heat flows were equated to give the unique values of T_{AL} and heat flow which satisfied both methods and the overall conductance calculated from this heat flow value.

It is considered that the resulting value of conductance is sufficiently accurate for our purpose since the assumed temperatures and air flow rates have been selected to be within the test range of variability and at the design point for the proposed insulation assembly.

3 Skin heat flow

(a) q_r/A , the radiative heat flow from the skin to the foil, can be expressed as:

$$q_r/A = \epsilon \sigma (T_S^4 - T_{AL}^4) .$$

For $T_S = 393^\circ\text{K}$ and $\epsilon = 0.04$ for aluminium foil facing painted aluminium this reduces to

Appendix 2

$$q_r/A = 9.54 - 0.04(T_{AL}/100)^4 \quad \text{CHU/ft}^2 \text{ hr} \quad (10)$$

(b) q_c/A , the convective heat flow from the skin to the foil can be expressed, under laminar natural convection, as

$$q_c/A = 0.21(N_{RA})^{1/4} (T_S - T_{AL}) \text{ kf/x}$$

where N_{RA} = Rayleigh Number

kf = air conductivity at film temperature T_f

x = distance from skin to foil.

Assuming ground level pressure, a film temperature of 115°C and $(T_S - T_{AL}) = \Delta T$ this reduces to

$$q_c/A = 0.224 \Delta T^{5/4} x^{-1/4} \quad \text{CHU/ft}^2 \text{ hr} \quad (11)$$

for x in inches.

(c) $q_{S''}/A$, the heat flow from the stringer to the foil, was assumed to be conductive in view of the small distance, x_1 , between the stringer flange and the foil.

Thus

$$q_{S''}/A = A_{S''} \Delta T \text{ kf}/x_1 \text{ A} \cdot$$

To allow for the stringer fin effect discussed in para 5.3.2 the stringer flange area $A_{S''}$ was increased by a factor of 1.1. This equation then reduces to

$$q_S/A = 0.0262 \Delta T x_1^{-1} \quad \text{CHU/ft}^2 \text{ hr} \quad (12)$$

The total heat flow from the skin to the aluminium foil is thus the sum of equations (10), (11) and (12) and since this heat also flows through the primary insulation it equals q_P/A .

Thus

$$q_P/A = 9.54 - 0.04(T_{AL}/100)^4 + 0.224 \Delta T^{5/4} x^{-1/4} + 0.0262 \Delta T x_1^{-1} \quad .$$

By inserting the appropriate values for x and x_1 the value of q_P/A can be calculated for a range of values of T_{AL} . The resultant values for specimen B198.4 are plotted in Fig.1.

4 Insulation heat flow

The rate of heat flow from the aluminium foil through the primary insulation can be expressed as

$$q_p/A = (T_{AL} - T_A)/R$$

where R is the thermal resistance of the composite assembly and

$$R = 1/h + \sum \ell/k$$

h = forced heat transfer coefficient in the duct calculated from McAdams⁴ equation

$$(h/C_p \text{ bG}) (\nu_p \mu/k)_b^{2/3} (\mu_w/\mu_b)^{0.14} = 0.23/(DG/\mu_p)^{0.2}$$

which applies for moderate values of ΔT with turbulent flow in ducts with L/D greater than 60. This gives a value of

$$h = 1.80 \quad \text{CHU/ft}^2 \text{ hr}^\circ\text{C}$$

for the assumed temperature and main flow condition. Using this value for h and appropriate values for ℓ and k (from Appendix 1) the value of R was calculated and values of q_p/A derived for a range of values of T_{AL} . The values obtained for specimen B198.4 are plotted in Fig.1.

5 Theoretical conductance

It can be seen in Fig.1 that the two curves intersect at $T_{AL} = 103^\circ\text{C}$ and that the corresponding value of q_p/A is $9.88 \text{ CHU/ft}^2 \text{ hr}$. Since the assumed skin temperature is 120°C and the air duct air temperature is 20°C the theoretical conductance of the primary insulation assembly in specimen B198.4 is

$$(k/\ell)F_{th} = 0.0988 \quad \text{CHU/ft}^2 \text{ hr}^\circ\text{C} .$$

The values for the other specimens were calculated in a similar manner and are listed in Table 1.

TABLE 1

Primary insulation heat flow rate and conductance

Test specimen No.	Heat flow up frame member $q_F/\ell\Delta T$ CHU/ft hr °C			Bulk insulation heat flow $q_F/A\Delta T$ CHU/ft ² hr °C	Equivalent conductance k'/ℓ CHU/ft ² hr °C	Theoretical conductance $(k/\ell)P_{th}$ CHU/ft ² hr °C	Heat and leakage factor $\frac{k'}{\ell}/k/\ell P_{th}$	Remarks
	4" frame	3" frame	2" frame					
1	-	0.0584	0.0566	0.0997	0.146	0.0993	1.47	Attachment in 2" frame
2	-	0.0595	0.0588	0.0993	0.147	0.097	1.52	Attachment in 2" frame
2H	-	0.0509	0.0483	0.1023	0.139	0.097	1.43	Added insulation above frames
3	-	0.0748	0.0291	0.104	0.143	0.0985	1.45	1.33 lb/ft min of duct air
3	-	0.109			0.166	0.0985	1.69	2.0 lb/ft min of duct air
3	-	0.1474			0.179	0.0985	1.82	2.67 lb/ft min of duct air
4	-	0.041	0.022	0.103	0.120	0.0988	1.22	
5	0.052	0.028	-	0.086	0.102	0.0745	1.38	
7	-	0.024	0.066	0.166	0.245	0.166	1.48	Panel buckled onto the 2" frame
6	0.06	0.025	-	-	-	-	-	Floor beam specimen

Values based on temperature difference between skin and air gap mean air temperature.

TABLE 2
Summary of results B198.1 test panel

Test No.	1	2	3	4	5	6	7	Arithmetic mean	Weighted mean
Air mass flow		6	6	8	4	6	8		
Air inlet temperature	20.3	20.55	18.75	20.75	33.75	33.08	30.99		
Skin temperature	126.98	118	118	120	121	118	123		
<u>Specimen heat balance</u>									
Power input	202	196	183	203	199	179	193	194	
Heat output	173.5	206	181	199	65.5	109	76	136	
Heat through flow	154	141.5	139	143	130.69	127.7	128.6	137	
<u>Specimen heat flow</u>									
Heat flow up 3" frame	0.0606	0.0625	0.0557	0.0603	0.0600	0.0544	0.0535	0.0581	0.0584
Heat flow up 2" frame	0.0508	0.0444	0.0540	0.0488	0.0659	0.0889	0.0564	0.0585	0.0566
Heat flow through primary insulation	0.1027	0.0997	0.0980	0.0991	0.0972	0.0995	0.1003	0.0995	0.0997
Equivalent conductance of primary insulation based on q_T	0.146	0.141	0.142	0.142	0.151	0.160	0.143	0.146	0.146

Theoretical value of primary insulation conductance from skin to mid air passage at 6 lb/min flow = $\left(\frac{k}{l}\right) P^{th}$

$$\left(\frac{k}{l}\right) P^{th} = 0.0993 \text{ CHU/ft}^2 \text{ hr } ^\circ\text{C}$$

Equivalent conductance from experimental results = k'/l

$$\frac{k'}{l} = 0.146 \text{ CHU/ft}^2 \text{ hr } ^\circ\text{C}$$

$$\text{Heat leakage factor} = \frac{\frac{k'}{l}}{\left(\frac{k}{l}\right) P^{th}} = \frac{0.146}{0.0993} = 1.47$$

TABLE 3

Summary of results B198.2 test panel

Test No.			1	2	3	4	5	6	7	8	Mean value	
			4	4	4	6	8	4	6	8	Arithmetic	Weighted
Air mass flow	M	lb/min	4	4	4	6	8	4	6	8		
Air inlet temp	T _{IN}	°C	19.8	20	20	20.6	17.2	30.9	28.1	32.3	23.6	
Skin temp	T _S	°C	119.9	117.3	119.3	119.6	121.7	122.5	122.2	122.2	120.6	
<u>Specimen heat balance</u>												
Power input	q _{IN}	CHU/hr	234	218	237	238	237	224	227	222	228	
Heat output	q _{OUT}	CHU/hr	168	149.5	155	179	215	130	142	213	173	
Heat through flow	q _T	CHU/hr	142	150	136	152	151	126	135	130.5	140	
<u>Specimen heat flow</u>												
Up 3" frame	q _p /l ΔT	CHU/ft hr°C	0.0597	0.0664	0.0534	0.0634	0.0582	0.0483	0.0612	0.0601	0.0588	0.0595
Up 2" frame	q _o /l ΔT	CHU/ft hr°C	0.0510	0.0641	0.0543	0.0702	0.0551	0.0597	0.0517	0.0627	0.0586	0.0588
Through primary insulation	q _p /A ΔT	CHU/ft ² hr°C	0.0991	0.0983	0.0989	0.1000	0.1014	0.1017	0.0980	0.0974	0.0994	0.0993
Conductance	k'/l	CHU/ft ² hr°C	0.143	0.153	0.140	0.156	0.145	0.143	0.142	0.148	0.146	0.147

Theoretical value of primary insulation conductance from skin to mid air passage at 6 lb/min flow = $(k/l)P_{th}$

$$(k/l)P_{th} = 0.097 \text{ CHU/ft}^2 \text{ hr}^\circ\text{C} .$$

Equivalent conductance from experimental results = k'/l .

$$k'/l = 0.147 \text{ CHU/ft}^2 \text{ hr}^\circ\text{C} .$$

$$\text{Heat leakage factor} = \frac{k'}{l} / (k/l)P_{th} = 1.52 = \text{CHU/ft}^2 \text{ hr}^\circ\text{C} .$$

TABLE 4 - Summary of results B198.2 modified test panel

Test No.			1	2	3	Arithmetic	Weighted
Air mass flow	\dot{M}	lb/min	4	6	8	mean	mean
Air inlet temp	T_{IN}	$^{\circ}C$	23	19	18.5	20.2	
Skin temp	T_S	$^{\circ}C$	125	118	121	121.3	
<u>Specimen heat balance</u>							
Power input	q_i	CHU/hr	232	222	237		
Heat output	q_o	CHU/hr	178	218	251		
Heat through flow	q_T	CHU/hr	140	131	140		
<u>Specimen heat flow</u>							
Heat flow up 3" frame	$q_p/\ell \Delta T$	CHU/ft hr $^{\circ}C$	0.0521	0.0471	0.0525	0.0506	0.0509
Heat flow up 2" frame	$q_c/\ell \Delta T$	CHU/ft hr $^{\circ}C$	0.0502	0.0476	0.0466	0.0481	0.0483
Heat flow through primary insulation	$q_p/A \Delta T$	CHU/ft 2 hr $^{\circ}C$	0.1019	0.1029	0.1022	0.1023	0.1023
Primary insulation conductance based on q_T	k'/ℓ	CHU/ft 2 hr $^{\circ}C$	0.140	0.137	0.139	0.139	0.139

Theoretical value of primary insulation conductance from skin to mid air passage at 6 lb/min flcw = $(k/\ell)P_{th}$

$$(k/\ell)P_{th} = 0.097 \text{ CHU/ft}^2 \text{ hr}^{\circ}C .$$

Equivalent conductance from experimental results = k'/ℓ

$$k'/\ell = 0.139 .$$

$$\text{Heat leakage factor} = \frac{k'/\ell}{(k/\ell)} P_{th} = \frac{0.139}{0.097} = 1.43 \text{ CHU/ft}^2 \text{ hr}^{\circ}C .$$

TABLE 5
 Summary of results B198.3 test panel

Test No.			1	2	3	4	5	6	1	2	3	4	5	6	7	Arithmetic mean		
Air mass flow	M	lb/min	4	6	8	4	6	8	4	6	8	4	6	8	8	4	6	8
Air inlet temp	T_{IN}	$^{\circ}C$	24.56	22.4	20.5	26.25	22.19	23.06	29.8	31.6	30.4	27.6	27.8	30.75	29.8	27	26	26.9
Skin temp	T_S	$^{\circ}C$	103.8	101.2	96.9	119.5	123.6	118	103.4	100.1	99.2	120.8	122.4	117.5	115.5	111.9	111.8	109.4
Specimen heat balance																		
Power input	q_{IN}	CHU/hr	196	222.2	275.6	188.7	251.4	288.7	178.3	200	252.7	231	251	277.4	280			
Heat output	q_{OUT}	CHU/hr	111.64	150.6	187.66	160.3	186.44	213.44	95.72	65.92	84.02	130.64	133.28	114.04	114.7			
Heat through flow	q_T	CHU/hr	117.16	137.95	158.15	149.72	194	221.26	111.33	141.73	145.71	141.54	175.25	205.59	160.6			
Specimen heat flow																		
Heat flow 3" frame	$\frac{q_T}{\ell \Delta T}$	CHU/ft hr $^{\circ}C$	0.07337	0.099	0.143	0.084	0.114	0.164	0.074	0.118	0.142	0.068	0.104	0.178	0.111	0.0748	0.109	0.1474
Heat flow 2" frame	$\frac{q_p}{\ell \Delta T}$	CHU/ft hr $^{\circ}C$	0.0214	0.0344	0.0213	0.0188	0.0321	0.0316	0.0326	0.0351	0.0281	0.0330	0.0318	0.0291	0.0281		0.0291	Mean for the three mass flows.
Heat flow primary insulation	$\frac{q_p}{A \Delta T}$	CHU/ft 2 hr $^{\circ}C$	0.1028	0.1021	0.0965	0.1079	0.1070	0.1022	0.1001	0.1019	0.1011	0.1076	0.1111	0.1058	0.1064		0.1040	
Equivalent conductance of primary insulation based on q_T	$\frac{k'}{\ell}$	CHU/ft 2 hr $^{\circ}C$	0.137	0.158	0.170	0.146	0.169	0.192	0.142	0.168	0.177	0.147	0.168	0.194	0.164	0.143	0.166	

Theoretical value of primary insulation conductance from skin to mid air passage at 6 lb/min flow = $\frac{k}{\ell} P_{th}$

$$\frac{k}{\ell} P_{th} = 0.0985 \text{ CHU/ft}^2 \text{ hr}^{\circ}C$$

Equivalent conductance from experimental result = $\frac{k'}{\ell}$

$$\frac{k'}{\ell} = \begin{matrix} 0.143 & \text{CHU/ft}^2 \text{ hr}^{\circ}C & \text{at 4 lb/min air flow} \\ 0.166 & \text{CHU/ft}^2 \text{ hr}^{\circ}C & \text{at 6 lb/min air flow} \\ 0.179 & \text{CHU/ft}^2 \text{ hr}^{\circ}C & \text{at 8 lb/min air flow} \end{matrix}$$

$$\text{Heat leakage factor} = \frac{k'}{\ell} / \frac{k}{\ell} P_{th} = \begin{matrix} 1.45 & \text{at 4 lb/min air flow} \\ 1.69 & \text{at 6 lb/min air flow} \\ 1.82 & \text{at 8 lb/min air flow} \end{matrix}$$

TABLE 6

Summary of results B198.4 (20' specimen) test panel

Test No.	COLD								HOT							
	1	2	3	4	5	6	7	8	9	10	11	12	13	14		
Air mass flow	M	lb/min	4	4(R)	4	4(R)	6	6	8	8	4	4	6	6	8	8
Air inlet temp	T_{IN}	$^{\circ}C$	20.7	18.06	23.5	21.94	23.31	22.0	25.31	23.19	32.56	30.25	27.5	30.87	32.19	29.64
Skin temp	T_S	$^{\circ}C$	104.02	101.08	122.47	120.72	103.9	117.94	102.7	118.99	109.85	118.3	104.71	117.41	105.69	118.27
Specimen heat balance																
Power input	q_{IN}	GHU/hr	136	137.7	167.2	174.7	132.7	159.3	130.7	166.6	129.7	149.5	132.7	149.6	126.7	152.5
Heat output	q_{OUT}	GHU/hr	136.8	128.5	169	163.1	118.7	165.5	114.7	159.5	113.9	142.1	134.5	125.8	131.2	141.2
Heat through flow	q_T	GHU/hr	100.2	95.1	119.6	117.1	94.9	111.7	82	121.2	90.6	105.5	97.8	109.6	93.7	112.6
Specimen heat flow																
Heat flow 3" frame	$\frac{q_F}{l \Delta T}$	GHU/ft hr $^{\circ}C$	0.043	0.039	0.040	0.036	0.036	0.038	0.032	0.047	0.041	0.040	0.047	0.045	0.049	0.046
															(mean)0.041	
Heat flow 2" frame	$\frac{q_o}{l \Delta T}$	GHU/ft hr $^{\circ}C$	0.023	0.008	0.024	0.018	0.036	0.018	0.009	0.024	0.018	0.024	0.029	0.027	0.023	0.026
															(mean)0.022	
Heat flow primary insulation	$\frac{q_p}{A \Delta T}$	GHU/ft 2 hr $^{\circ}C$	0.100	0.103	0.105	0.109	0.100	0.104	0.100	0.103	0.100	0.104	0.102	0.105	0.103	0.105
															(mean)0.103	
Equivalent conductance of primary insulation (based on q_T)	k'/l	GHU/ft 2 hr $^{\circ}C$	0.119	0.112	0.122	0.119	0.123	0.117	0.105	0.125	0.116	0.121	0.126	0.126	0.125	0.126
															(mean)0.120	

Theoretical value of primary insulation conductance from skin to mid air passage at 6 lb/min flow = $k/l P_{th}$

$$k/l P_{th} = 0.0988 \text{ GHU/ft}^2 \text{ hr}^{\circ}C .$$

Equivalent conductance from experimental results = k'/l

$$k'/l = 0.120 \text{ GHU/ft}^2 \text{ hr}^{\circ}C .$$

$$\text{Therefore heat leakage factor} = \frac{k'/l}{(k/l)P_{th}} = \frac{0.120}{0.0988} = 1.22 .$$

TABLE 7

Summary of results B198.5 test panel

Test No.			20°C inlet (nominal)			30°C inlet (nominal)			20°C inlet (nominal)			30°C inlet (nominal)			Arith- netic mean
			1	2	3	4	5	6	7	8	9	10	11	12	
Air mass flow	M	lb/min	4	6	8	4	6	8	4	6	8	4	6	8	
Air inlet temp	T _{IN}	°C	20.4	19.2	18.75	27.7	29.1	26.75	21.44	19.5	20.4	26.1	29.7	28.75	
Skin temp	T _S	°C	98.8	102.1	102.7	101.5	99.4	99.0	124.5	122.6	119.4	122.8	123	122.6	
<u>Specimen heat balance</u>															
Power input	q _{IN}	CHU/hr	140	148	156	111	123	127.5	178	177	195	153	173	177	
Heat output	q _{OUT}	CHU/hr	102.9	134	151	60.7	48.2	59.5	154.4	172.5	171	121	82	92	
Heat through flow	q _T	CHU/hr	80	96.7	92	76.9	79	84.4	106	108.8	109.6	104.8	96.6	94.9	
<u>Specimen heat flow</u>															
Heat flow 4" frame	q _p /l ΔT	CHU/ft hr°C	0.046	0.061	0.057	0.049	0.057	0.062	0.046	0.049	0.054	0.054	0.048	0.046	0.052
Heat flow 3" frame	q _p /l ΔT	CHU/ft hr°C	0.021	0.029	0.02	0.03	0.031	0.031	0.03	0.028	0.031	0.027	0.028	0.026	0.028
Heat flow primary insulation	q _p /A ΔT	CHU/ft ² hr°C	0.085	0.087	0.086	0.084	0.084	0.085	0.086	0.087	0.087	0.085	0.085	0.085	0.086
Equivalent conductance of primary insulation (based on q _T)	k'/l	CHU/ft ² hr°C	0.100	0.108	0.101	0.101	0.106	0.108	0.100	0.101	0.106	0.102	0.099	0.097	0.102

Theoretical value of primary insulation conductance from skin to mid air passage
 at 6 lb/min flow = $k/l P_{th}$

$$(k/l)P_{th} = 0.0745 \text{ CHU/ft}^2 \text{ hr}^\circ\text{C} .$$

Equivalent conductance from experimental results = k'/l

$$k'/l = 0.102 \text{ CHU/ft}^2 \text{ hr}^\circ\text{C} .$$

$$\text{Therefore heat leakage factor} = k'/l / (k/l)P_{th} = \frac{0.102}{0.074} = 1.38 .$$

TABLE 8
 Summary of results panel B198.7 test panel

			Cold						Hot						
Test No.			1	2	3	4	5	6	7	8	9	10	11	12	Mean (arith)
Air mass flow	M	lb/min	4	4	6	6	8	8	4	4	6	6	8	8	
Air inlet temp	T _{IN}	°C	23.6	21	23.2	18.7	21.2	19.9	28	26	24.9	26.7	27.2	29.3	
Skin temp	T _S	°C	98.7	114.3	96	112.2	98.6	114.5	98.4	117.64	98.3	117.45	95.37	115.3	
<u>Specimen heat balance</u>															
Power input	q _{IN}	CHU/hr	189.6	253	195.6	266.8	199	285	184.6	248	198	257.9	185.8	274.7	
Heat output	q _{OUT}	CHU/hr	122.76	167.1	109.19	160.34	121.75	160.16	120.38	178.4	111.38	169.34	102.19	142.36	
Heat through flow	q _T	CHU/hr	153.9	199.3	153.7	194.5	164	211.3	145.4	196.8	157.5	203.4	153.3	200.5	
<u>Specimen heat flow</u>															
Heat flow 3" frame	q _F /l ΔT	CHU/ft hr°C	0.024	0.029	0.025	0.019	0.026	0.026	0.019	0.020	0.025	0.030	0.023	0.026	0.024
Heat flow 2" frame	q _C /l ΔT	CHU/ft hr°C	0.062	0.052	0.069	0.063	0.065	0.074	0.066	0.062	0.069	0.063	0.074	0.076	0.066
Heat flow primary insulation	q _P /A ΔT	CHU/ft ² hr°C	0.22	0.23	0.23	0.23	0.23	0.24	0.23	0.24	0.23	0.24	0.24	0.25	0.23
Equivalent conductance of primary insulation (based on q _T)	k'/l	CHU/ft ² hr°C	0.232	0.238	0.240	0.237	0.239	0.253	0.236	0.245	0.243	0.251	0.256	0.264	0.245

Theoretical value of primary insulation conductance from skin to mid air passage at 6 lb/min flow

$$= k/l P_{th} = 0.166 \text{ CHU/ft}^2 \text{ hr}^\circ\text{C} .$$

Equivalent conductance from experimental results

$$= k'/l = 0.245 \text{ CHU/ft}^2 \text{ hr}^\circ\text{C} .$$

Therefore heat leakage factor $\frac{k'/l}{(k/l)P_{th}} = \frac{0.245}{0.166} = 1.48 .$

TABLE 9 - Summary of results panel B198.6

Floor beam specimens

Standard panel			20°C inlet (nominal)							30°C inlet (nominal)					
Test No.			1	2	3	4	5	6	7	8	9	10	11	12	13
Cooling air mass flow	M	lb/min	4	6	6	8	4	6	8	4	6	8	4	6	8
Skin temperature	T _S	°C	101.2	100.2	97.1	98	116.3	120.9	118.3	99.2	98.8	95.7	120.4	120.4	117
Cabin air temperature	T _{cab}	°C	23.2	24	23.6	24.4	25.3	22.75	22.5	23.5	25.5	27.6	23.5	25.6	28.8
Overall temperature difference (skin to cabin air)	ΔT'	°C	77.9	76.2	73.5	73.6	91	97.1	95.2	75.7	73.3	78.1	96.9	94.8	88.2
Mean air gap temperature	T _{air}	°C	23.8	23.6	23.6	25	25.8	21.5	21.1	29	31	31.2	33.4	30.9	34.1
Temperature difference (skin to air gap)	ΔT	°C	77.4	76.6	73.5	73	90.5	99.4	97.2	90.2	67.8	64.5	87	89.5	82.9
Total heat input	q _{IN}	CHU/hr	184	286	279	307	280	340	415	254	246	284	300	338	360
Total heat output	q _o	CHU/hr	169.9	177.8	179.7	201.7	188.6	267.7	257.2	139.6	110.6	120.0	165.2	166.8	108.6
Heat flow up main beam	q _B /ΔT'	CHU/hr°C	0.227	0.259	0.259	0.221	0.209	0.245	0.243	0.215	0.241	0.209	0.207	0.239	0.220
Heat flow up 4" frame	q _F /e ΔT	CHU/ft hr°C	0.0712	0.0692	0.0721	0.0808	0.0666	0.0946	0.85	0.0484	0.0413	0.1132	0.0529	0.0749	0.1037
Heat flow up 3" frame	q _o /e ΔT	CHU/ft hr°C	0.0206	0.0209	0.0204	0.034	0.0177	0.0392	0.0535	0.0271	0.0295	0.0388	0.0276	0.0313	0.0501
Heat flow up longeron	q _L /e ΔT	CHU/ft hr°C	0.1303	0.197	0.194	0.245	0.128	0.181	0.269	0.147	0.202	0.246	0.124	0.178	0.235
Heat flow up longeron	q _L '/e ΔT	CHU/ft hr°C	0.114	0.133	0.133	0.146	0.105	0.114	0.136	0.128	0.140	0.152	0.107	0.126	0.151
Modified panel			20°C inlet (nominal)							30°C inlet (nominal)					
Test No.			1	2	3	4	5	6	7	8	9	10	11	12	
Cooling air mass flow	M	lb/min	4	6	8	4	6	8	4	6	8	4	6	8	
Skin temperature	T _S	°C	101	93.5	93	123.3	120.1	119.5	104.2	104.5	100.2	121.9	119	114.5	
Cabin air temperature	T _{cab}	°C	27.2	27.6	27.8	24.8	25	26.2	28.8	28.3	28.1	28.6	28.5	28.2	
Overall temperature difference (skin to cabin air)	ΔT'	°C	73.8	65.9	65.2	98.5	95.1	93.3	75.4	76.2	72.1	93.3	90.5	86.3	
Mean air gap temperature	T _{air}	°C	27.7	27.4	27.5	26.5	25.5	25.4	33	35.3	33.1	36.7	35.6	35.2	
Temperature difference (skin to air gap)	ΔT	°C	73.3	66.1	65.5	96.8	94.6	94.1	71.2	69.2	67.1	85.2	83.4	79.3	
Total heat input	q _{IN}	CHU/hr	240	250	291	333	344	451	222	260	292	284	330	368	
Total heat output	q _o	CHU/hr	123.1	107.9	106.4	175.1	175.6	175.5	117.5	67.4	60.6	115.2	80.7	50.4	
Heat flow up main beam	q _B /ΔT'	CHU/hr°C	0.291	0.279	0.258	0.260	0.254	0.277	0.276	0.262	0.239	0.264	0.256	0.263	
Heat flow up 4" frame	q _F /e ΔT	CHU/ft hr°C	0.0818	0.0908	0.1451	0.1064	0.0814	0.1010	0.0477	0.0766	0.1654	0.0610	0.0719	0.1299	
Heat flow up 3" frame	q _o /e ΔT	CHU/ft hr°C	0.0982	0.1089	0.1161	0.0992	0.1142	0.1106	0.1123	0.0983	0.1028	0.1127	0.1055	0.1261	
Heat flow up longeron	q _L /e ΔT	CHU/ft hr°C	0.0941	0.1120	0.1420	0.0888	0.1036	0.1265	0.0772	0.0997	0.1311	0.0798	0.1007	0.1236	
Heat flow up longeron	q _L '/e ΔT	CHU/ft hr°C	0.1105	0.1165	0.1420	0.094	0.1078	0.1265	0.0955	0.1055	0.1103	0.0974	0.1103	0.1362	

TABLE 10

Heat flow up frame members

Heat flow based on one equivalent square foot of fuselage with outer skin at 120°C and cooling air, in integral air duct at 20°C.

Specimen	Total heat flow CHU/hr	Frame heat flow						Both frames % total
		4"		3"		2"		
		CHU/hr	% of total	CHU/hr	% of total	CHU/hr	% of total	
1	14.6			3.18	21.8	3.1	21.2	43
2	14.7			3.24	22	3.2	21.8	43.8
2M	13.9			2.77	19.9	2.63	18.9	38.8
3	14.3			4.07	28.5	1.59	11.1	39.6
3	16.6			5.95	35.8	1.59	9.6	45.4
3	17.9			8.05	45	1.59	8.9	53.9
4	12.0			2.24	18.7	1.2	10	28.7
5	10.2	2.84	27.8	1.53	15	-		42.8
7	24.5			1.31	5.5	3.6	14.6	20.1
6	-	3.41 to 5.11	-	1.36 to 2.36	-			
6M		3.75 to 6	-	6	-			

CONDUCTIVITY $\text{CHU}/\text{ft}^2 \text{hr. } ^\circ\text{C}/\text{in.}$

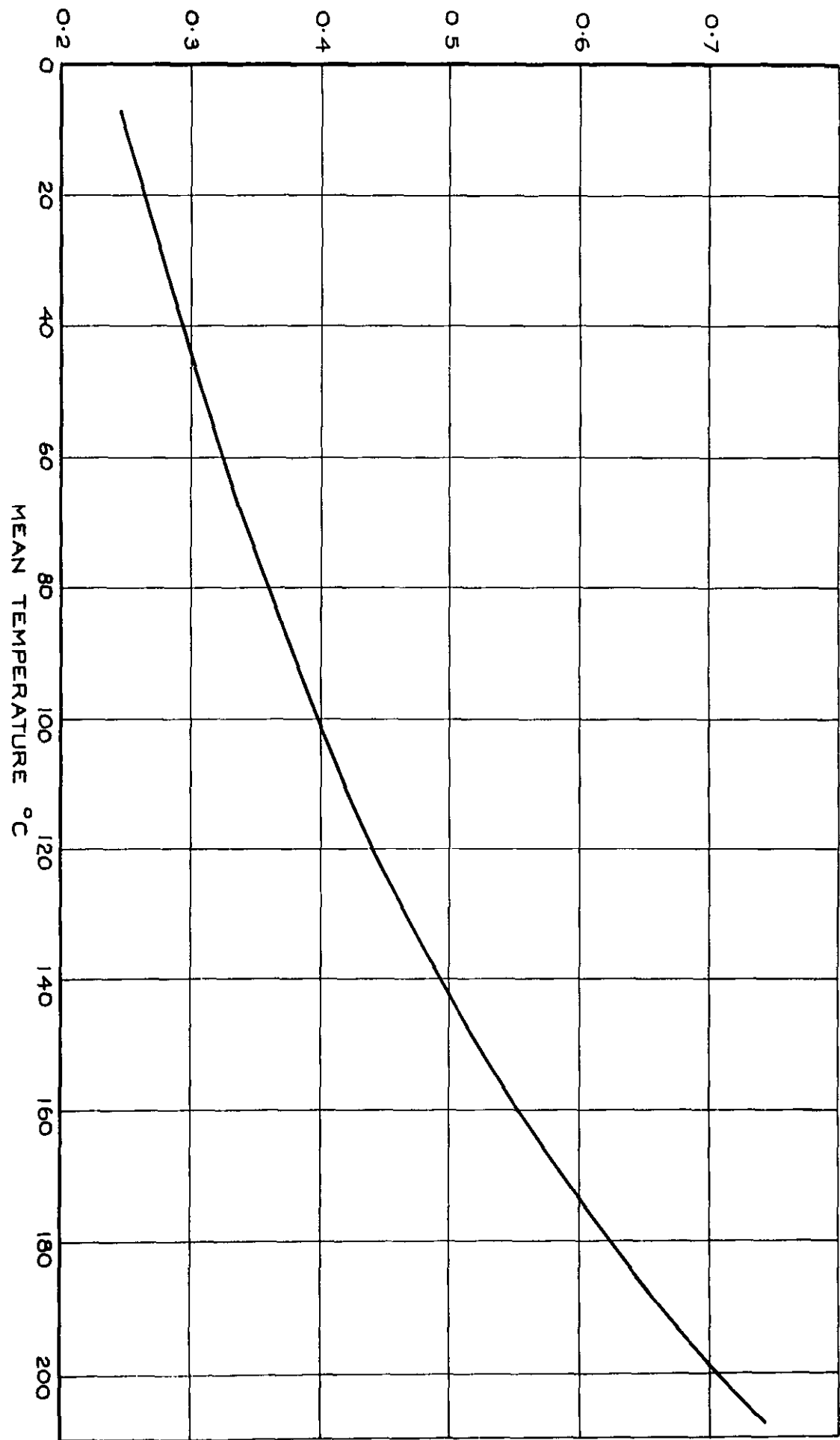


FIG.1. CONDUCTIVITY OF L.O.F. MICROLITE GLASS FIBRE.

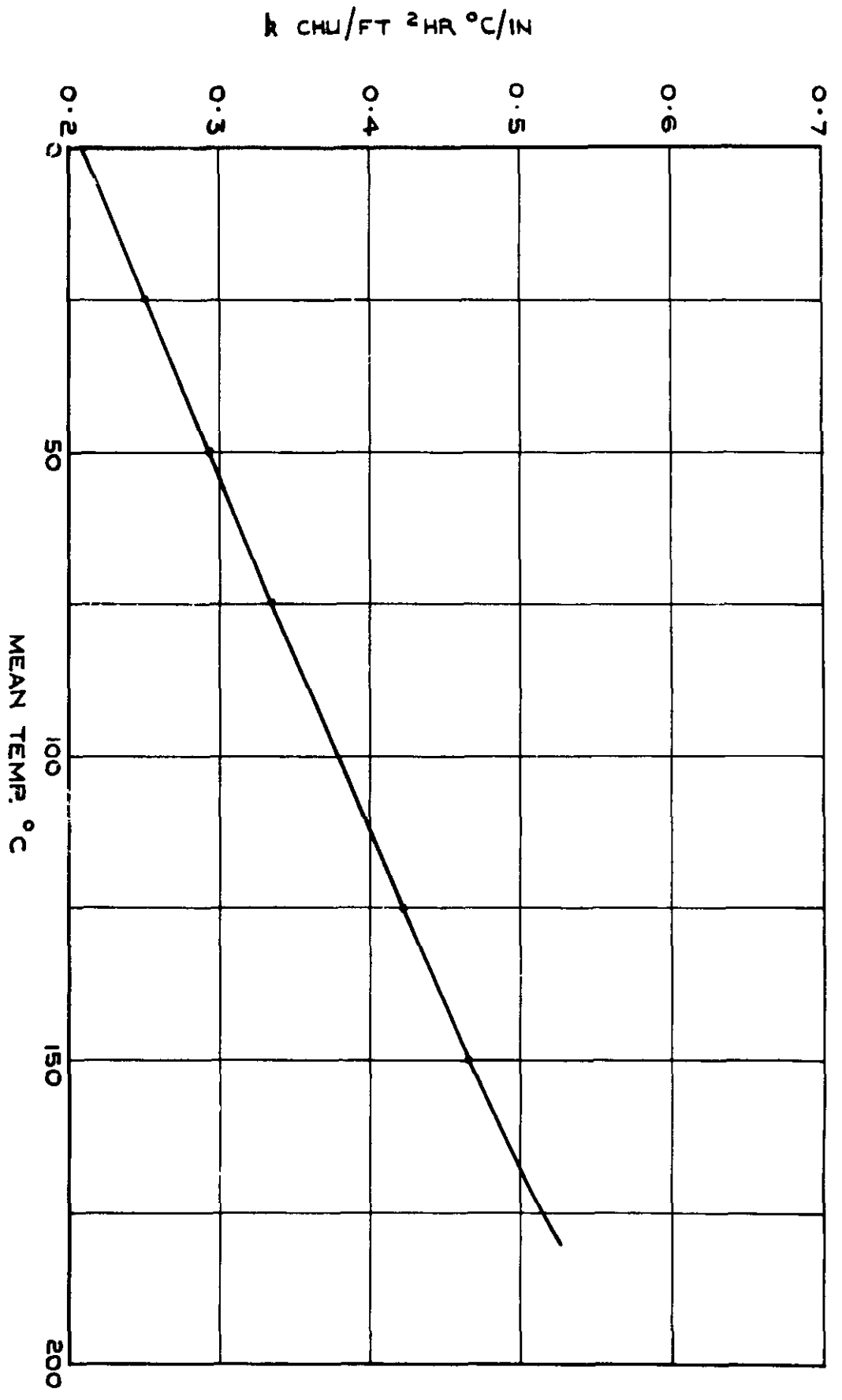


FIG.2. CONDUCTIVITY OF FIBREGLASS BLANKET

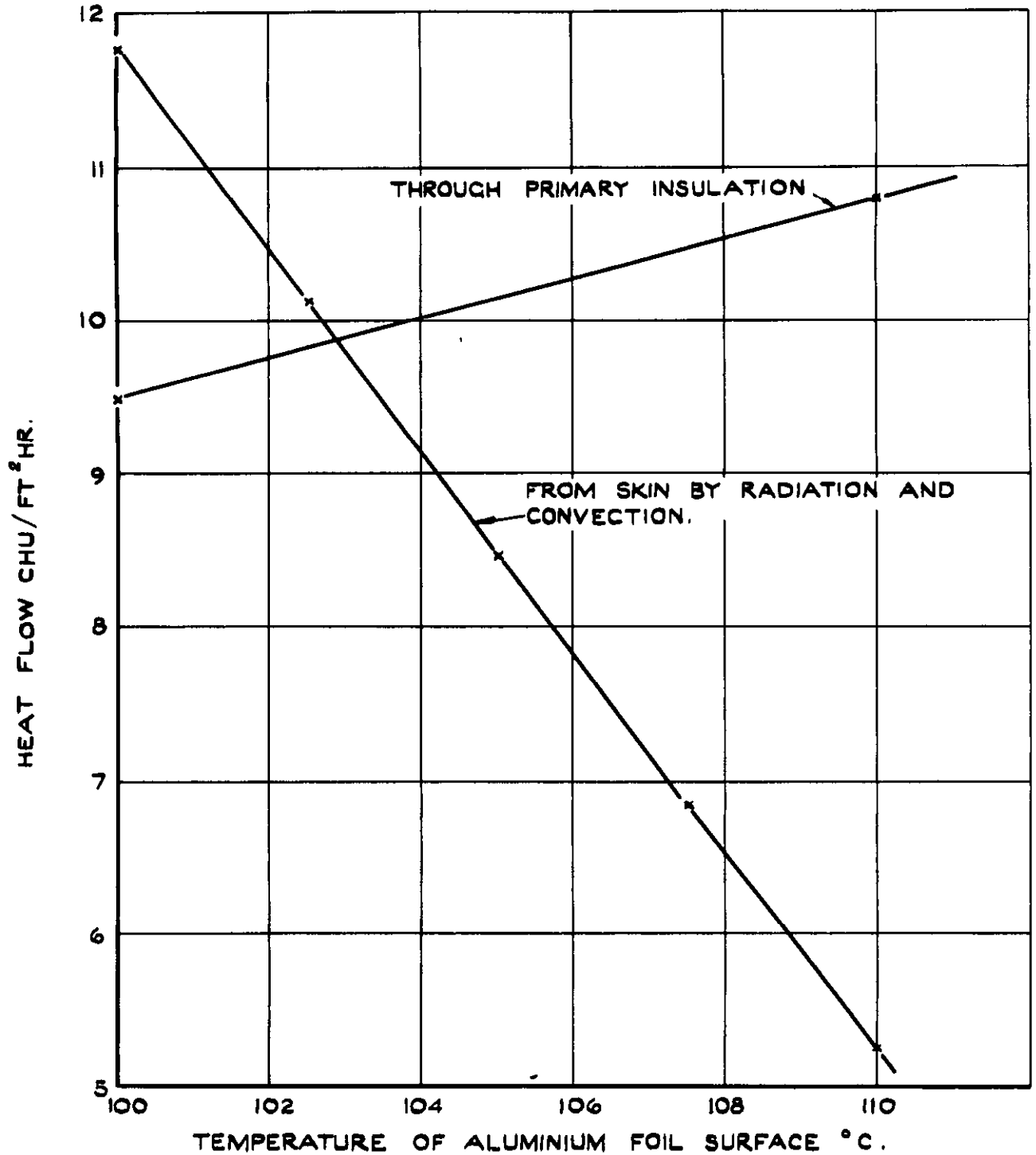


FIG.1. HEAT FLOW FROM STRUCTURE TO BULK PRIMARY INSULATION FOR $T_s = 120^{\circ}\text{C}$ $T_a = 20^{\circ}\text{C}$ PANEL B198 :4.

A TYPICAL BRISTOL 198 TEST SPECIMEN
INCORPORATING COOLING AIR DUCT
WITHIN THE INSULATION

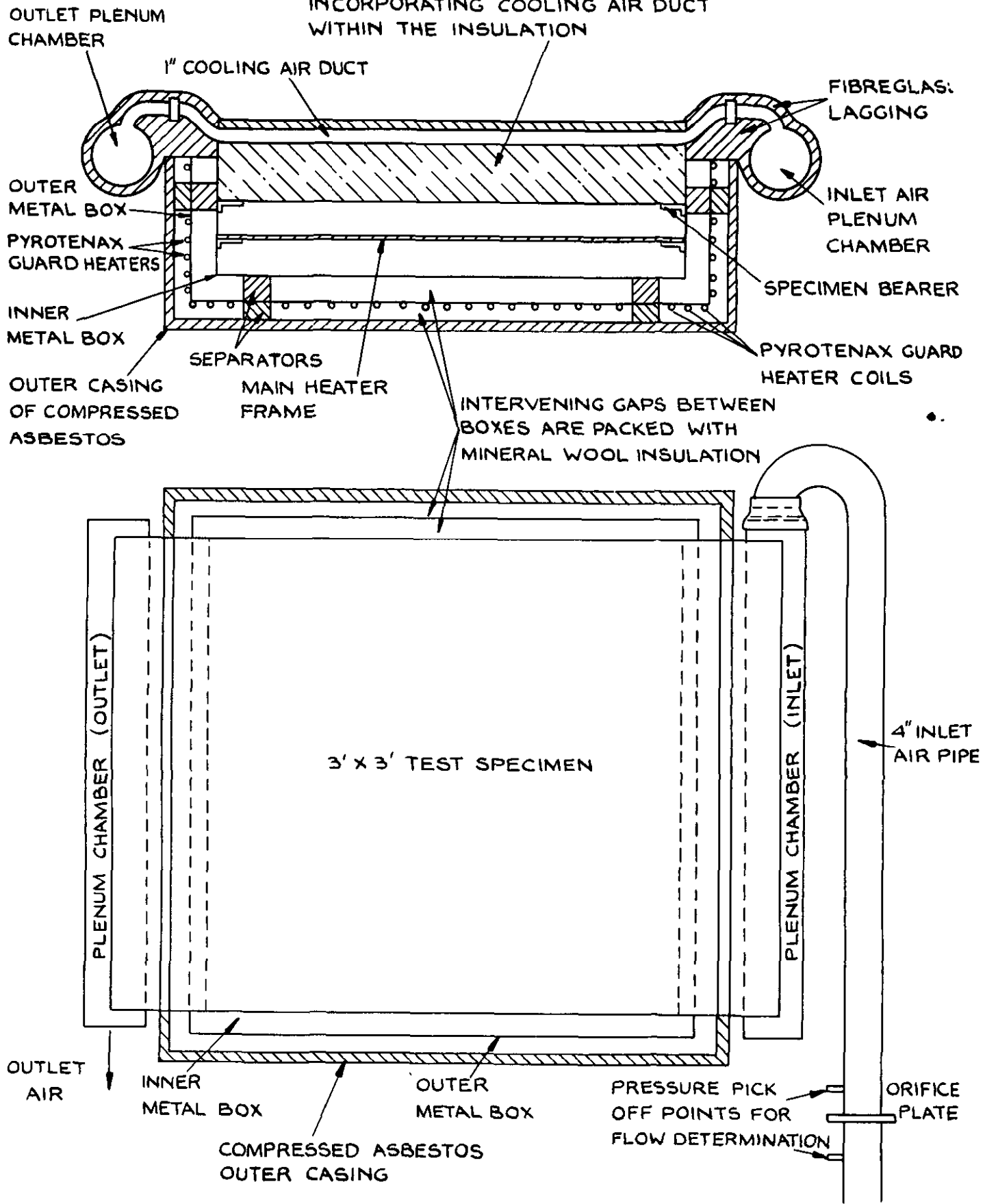


FIG. I. DIAGRAM OF THE THERMAL CONDUCTION TEST RIG



FIG.2 THERMAL CONDUCTION TEST RIG ASSEMBLY DETAILS

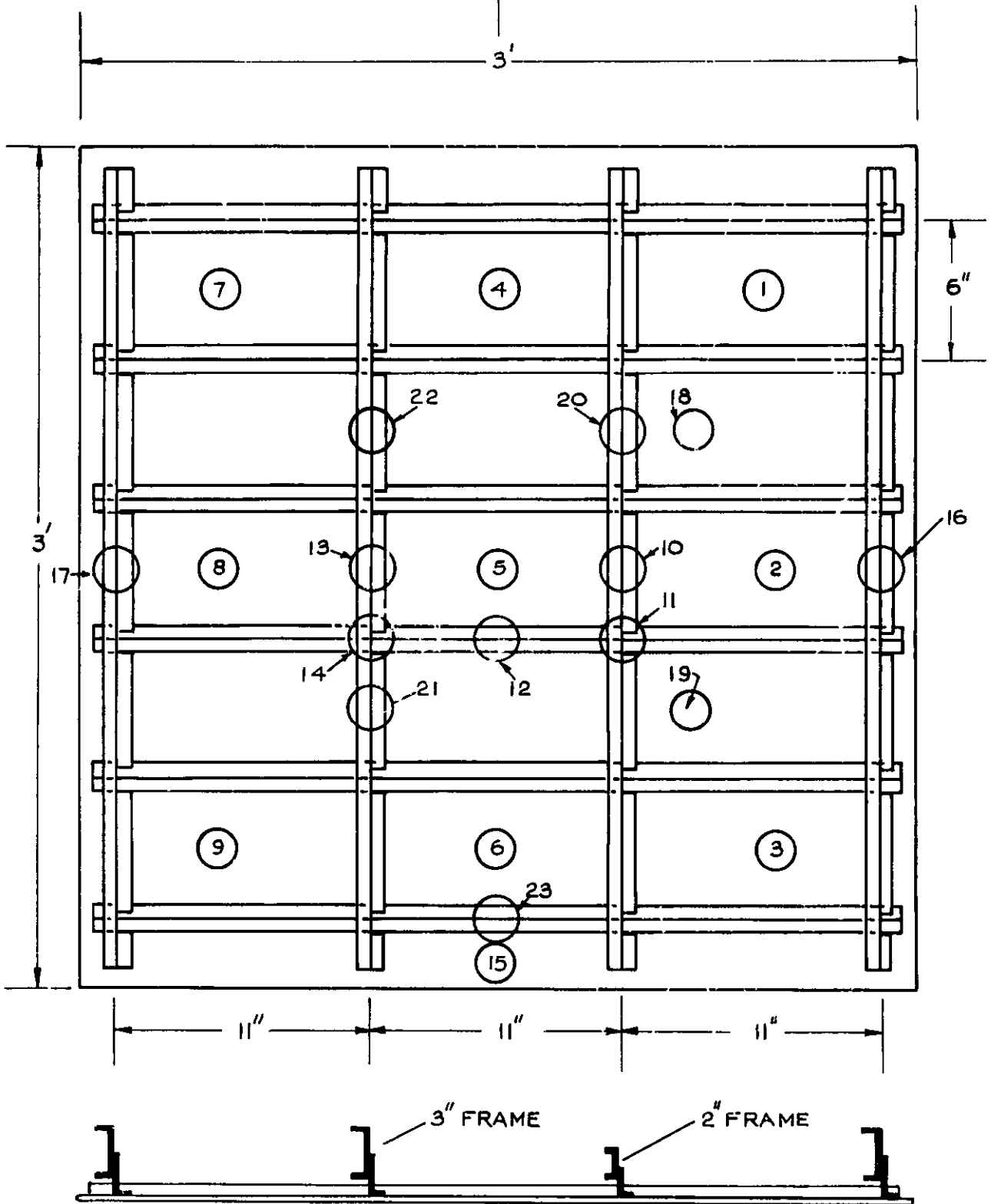


FIG.3. DETAILS OF PANEL STRUCTURE & LOCATION OF THERMOCOUPLE STATIONS: PANEL B198.1

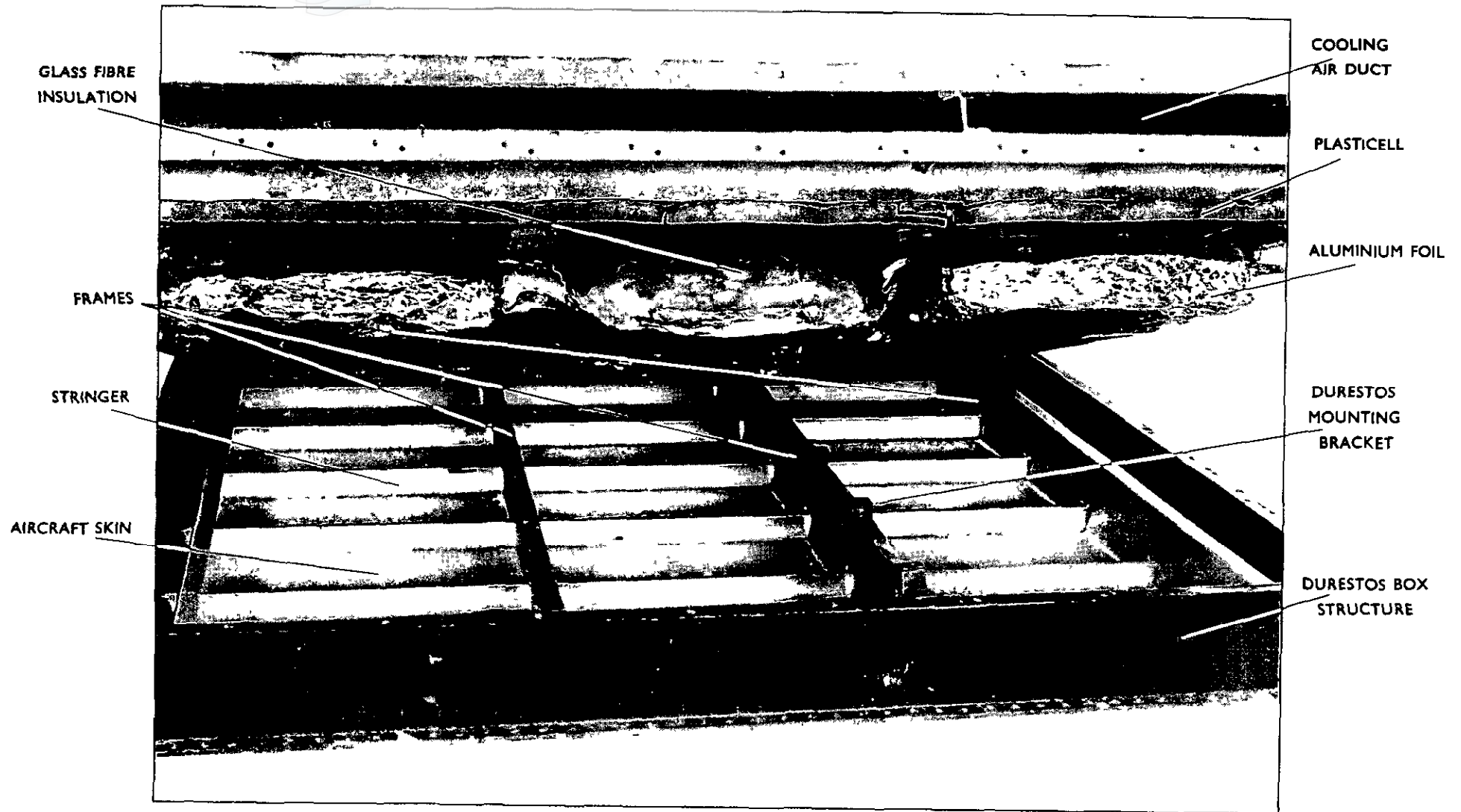
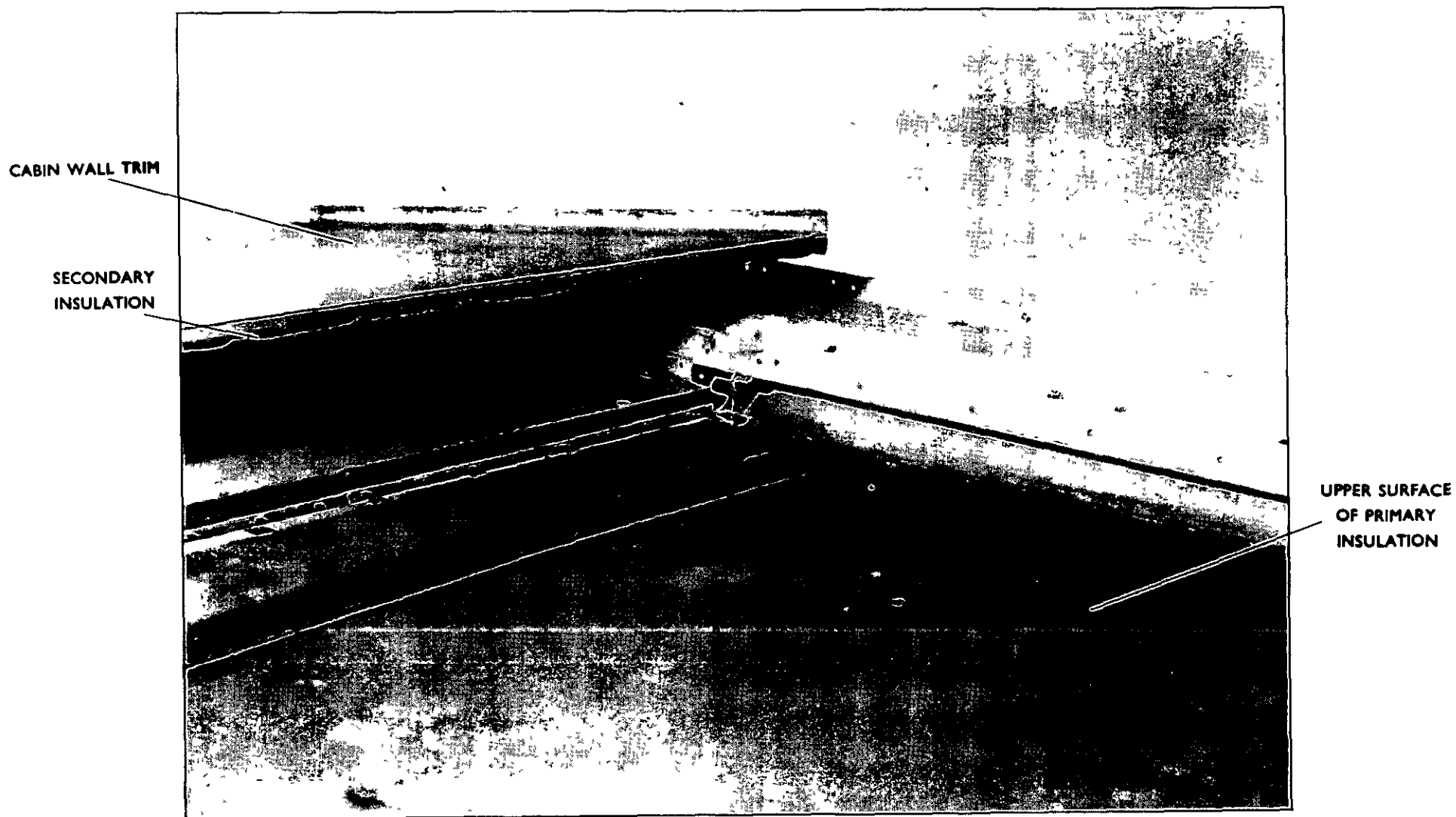


FIG.4. DETAIL OF A TYPICAL BRISTOL 198 TEST PANEL
AFTER TESTING



**FIG.5. TYPICAL BRISTOL 198 TEST PANEL (AFTER TESTING)
SHOWING SECONDARY INSULATION REMOVED TO REVEAL COOLING AIR DUCT**

X X POSITION OF AIR TEMP.
MEASURING THERMOCOUPLES
OR SCREENS. SITED WITHIN
AIR DUCT

UPPER SURFACE
OF SECONDARY
INSULATION
(CABIN WALL)

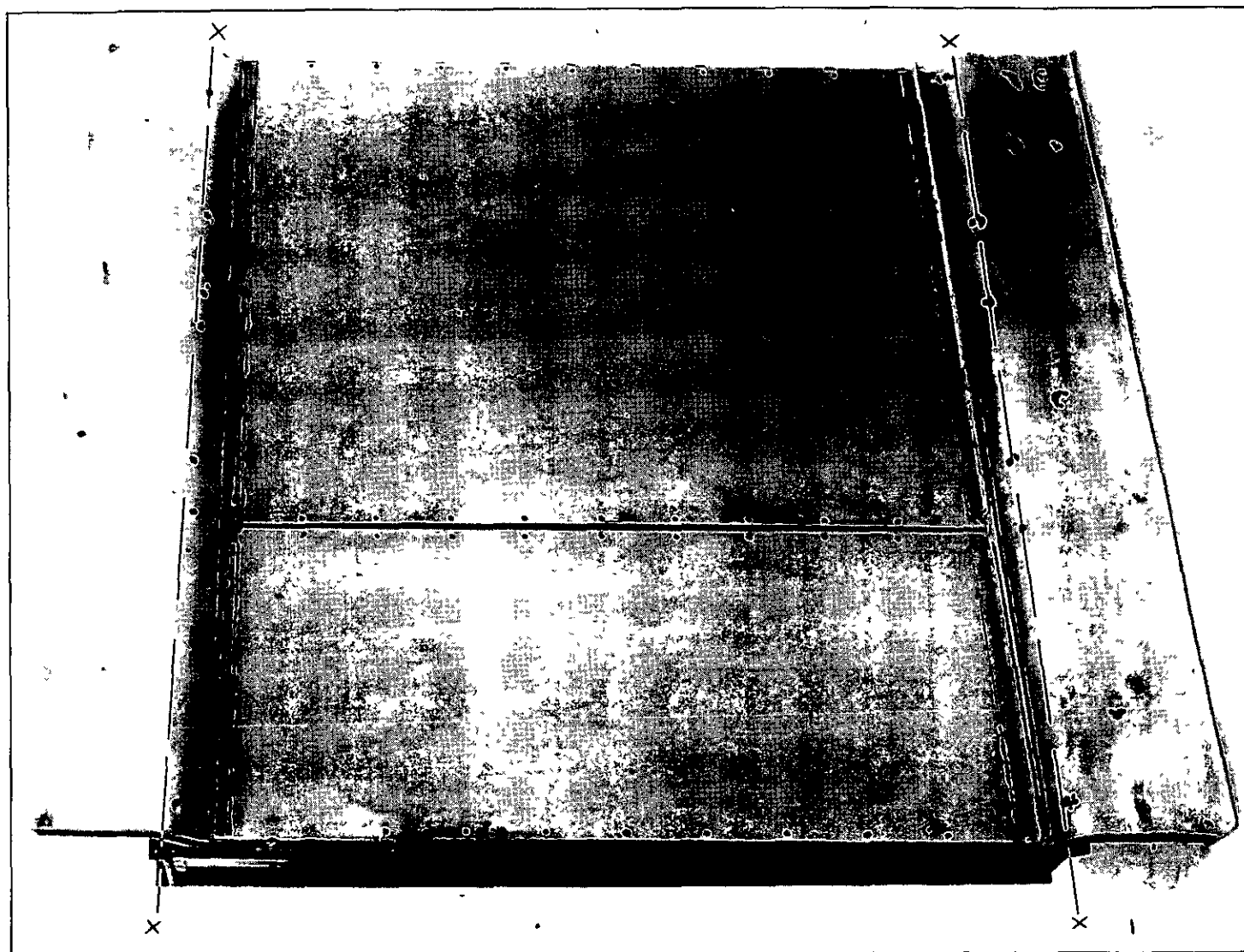


FIG.6. TYPICAL BRISTOL 198 TEST PANEL (VIEWED FROM ABOVE)

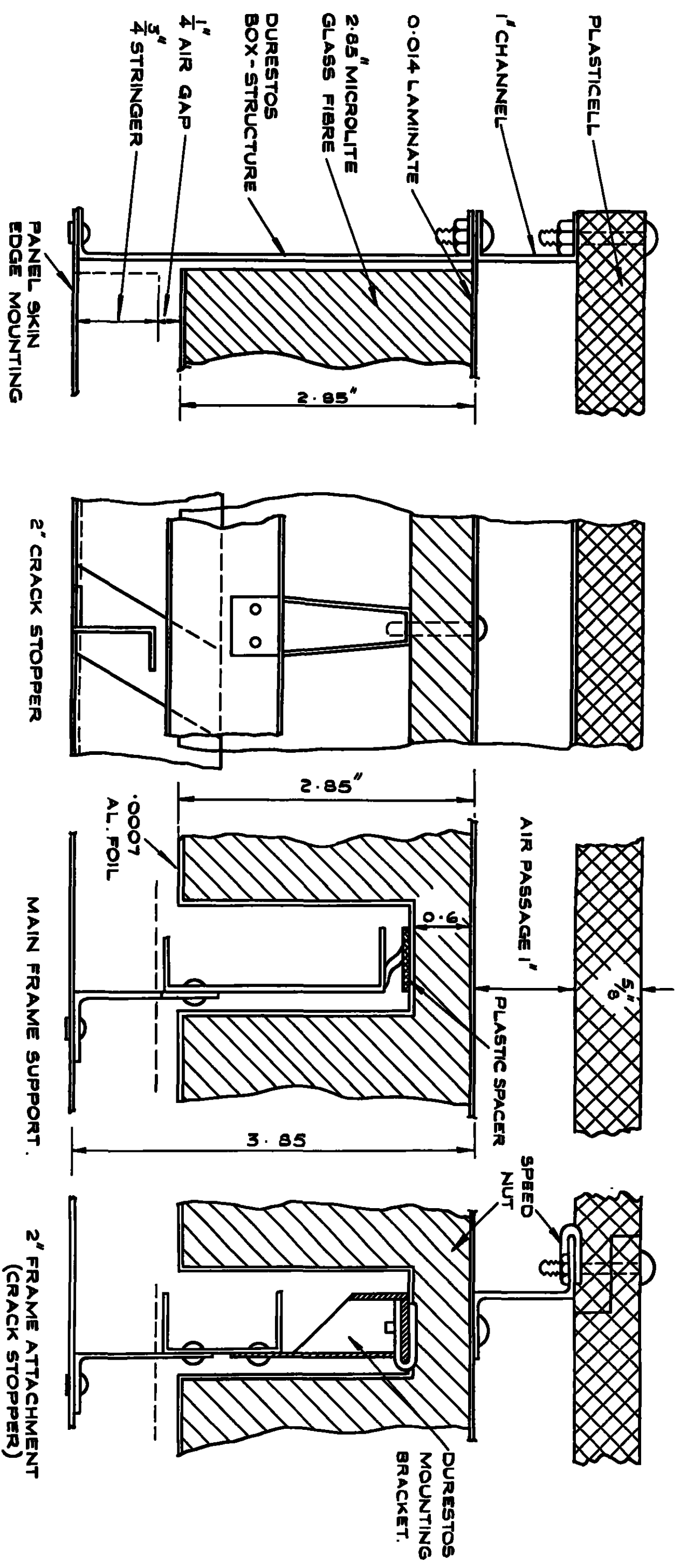


FIG. 7. DETAILS OF ATTACHMENT OF INSULATION TO STRUCTURE : PANEL B.198-1

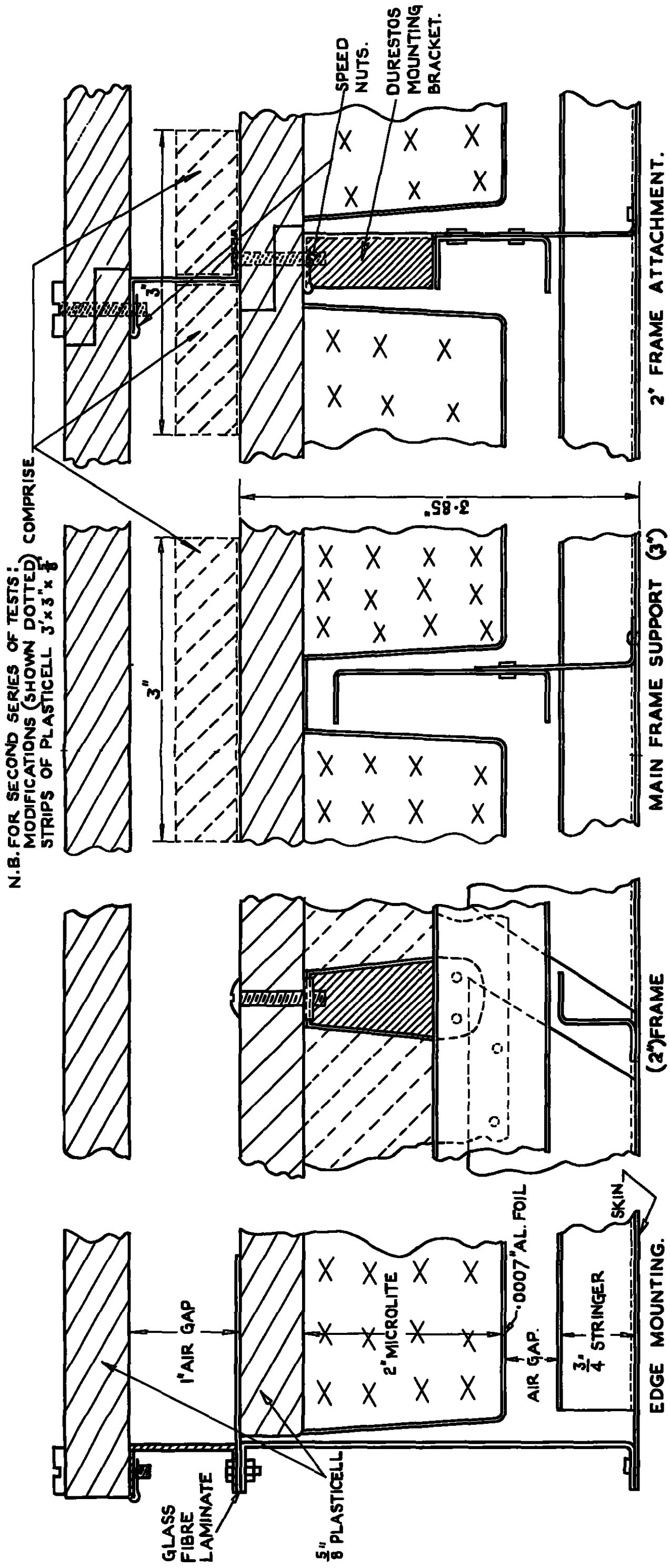


FIG.8. DETAILS OF ATTACHMENT OF INSULATION TO STRUCTURE.
 PANEL B 198.2 AND B 198.2 (MODIFIED)

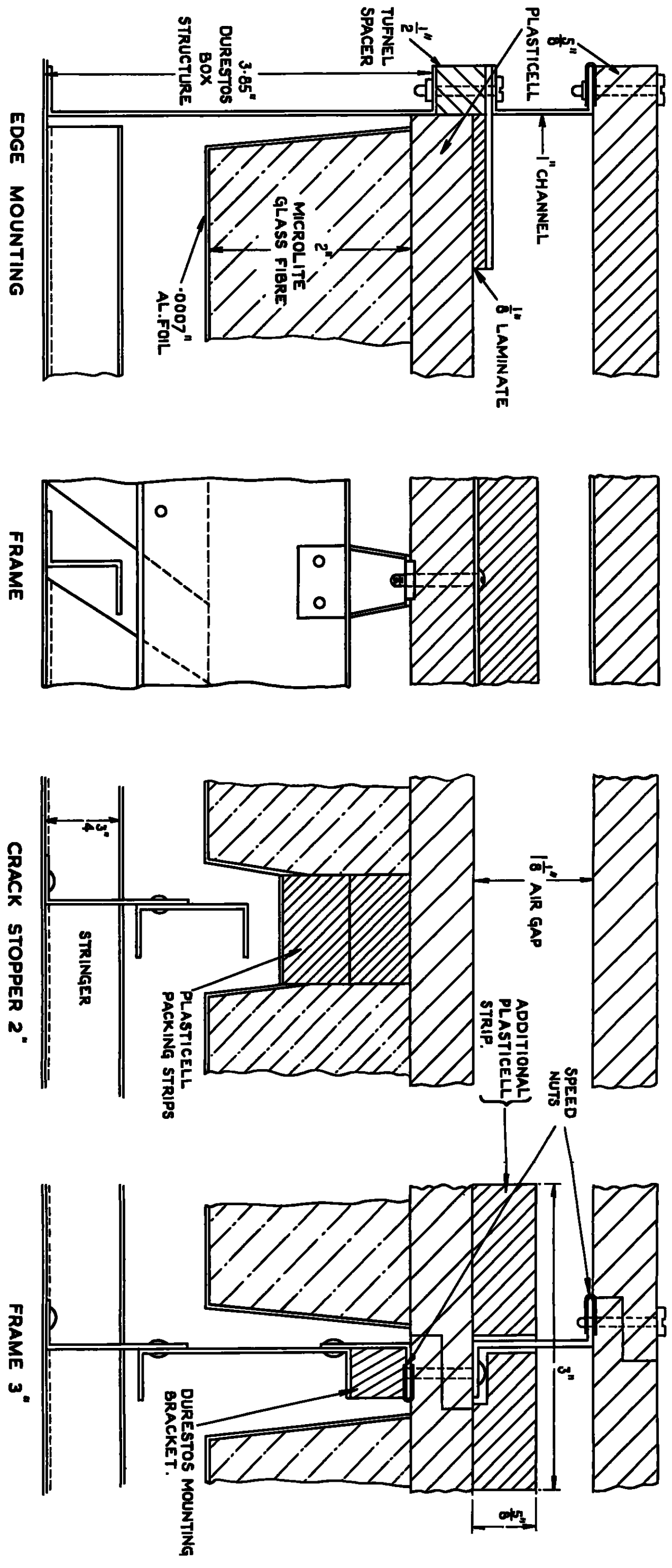


FIG. 9. DETAILS OF ATTACHMENT OF INSULATION TO STRUCTURE. PANEL B.198-3.

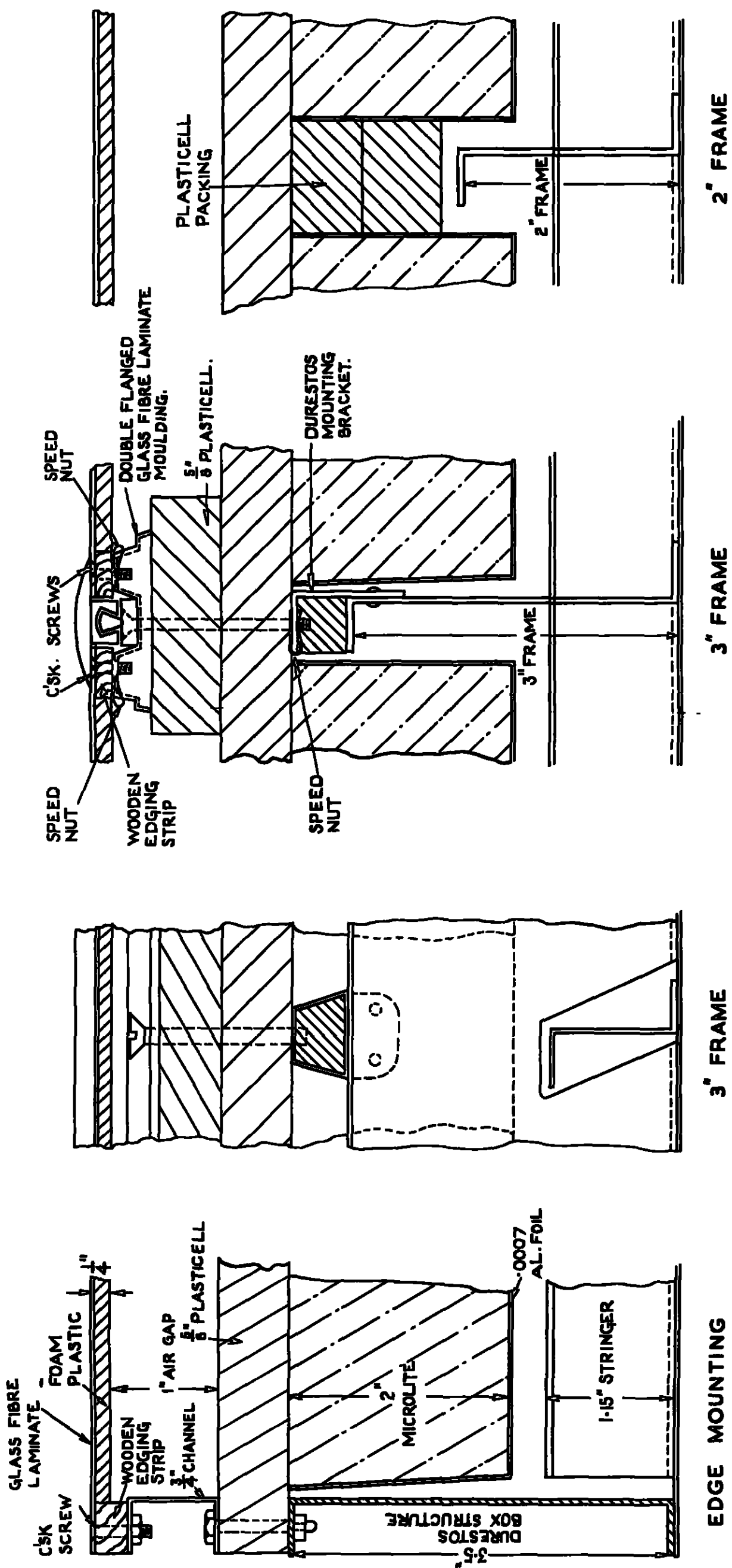


FIG. 10 DETAILS OF ATTACHMENT OF INSULATION TO STRUCTURE . PANEL B 198:4

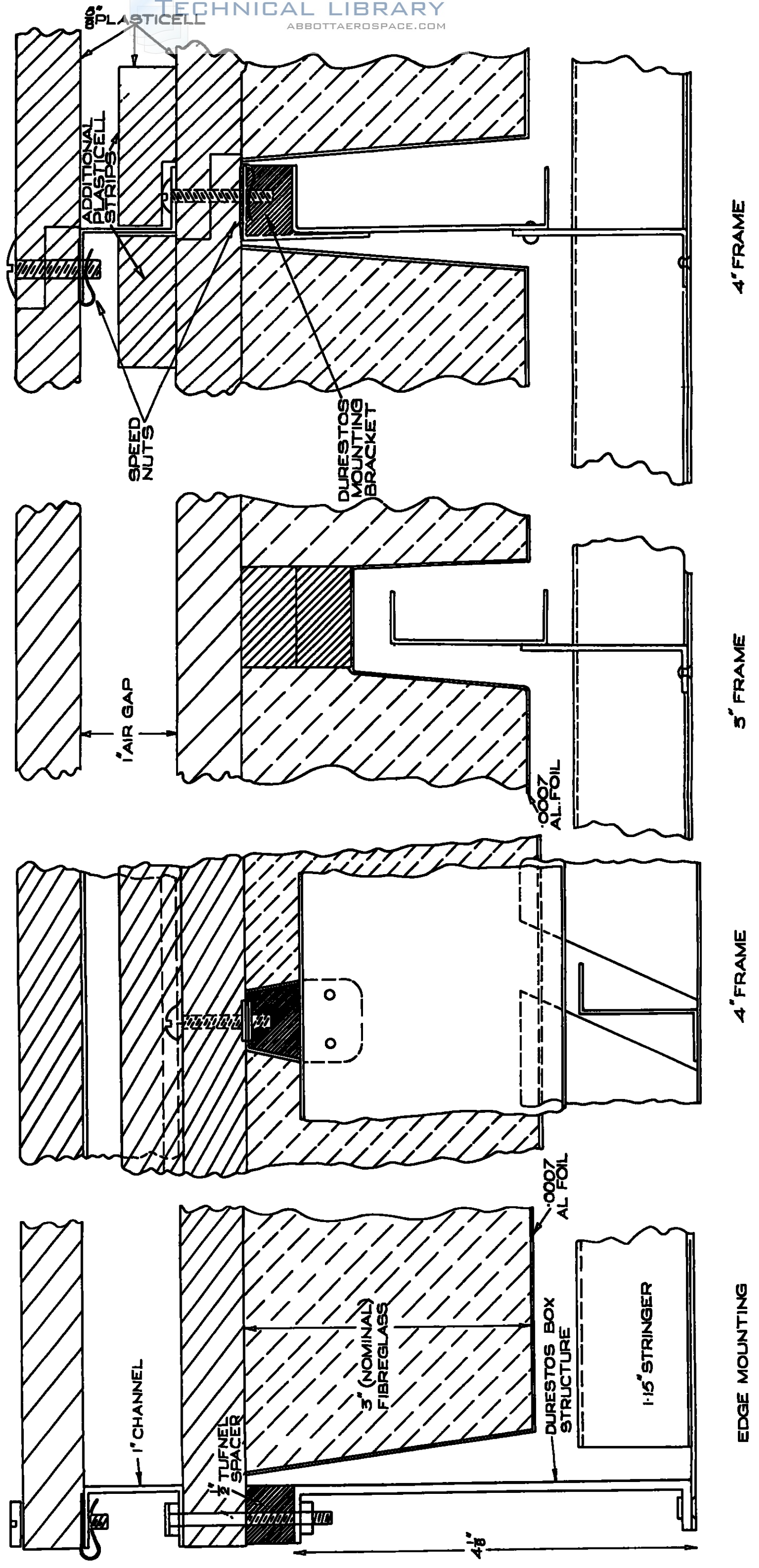


FIG.11. DETAILS OF ATTACHMENT OF INSULATION TO STRUCTURE. PANEL B.198-5.

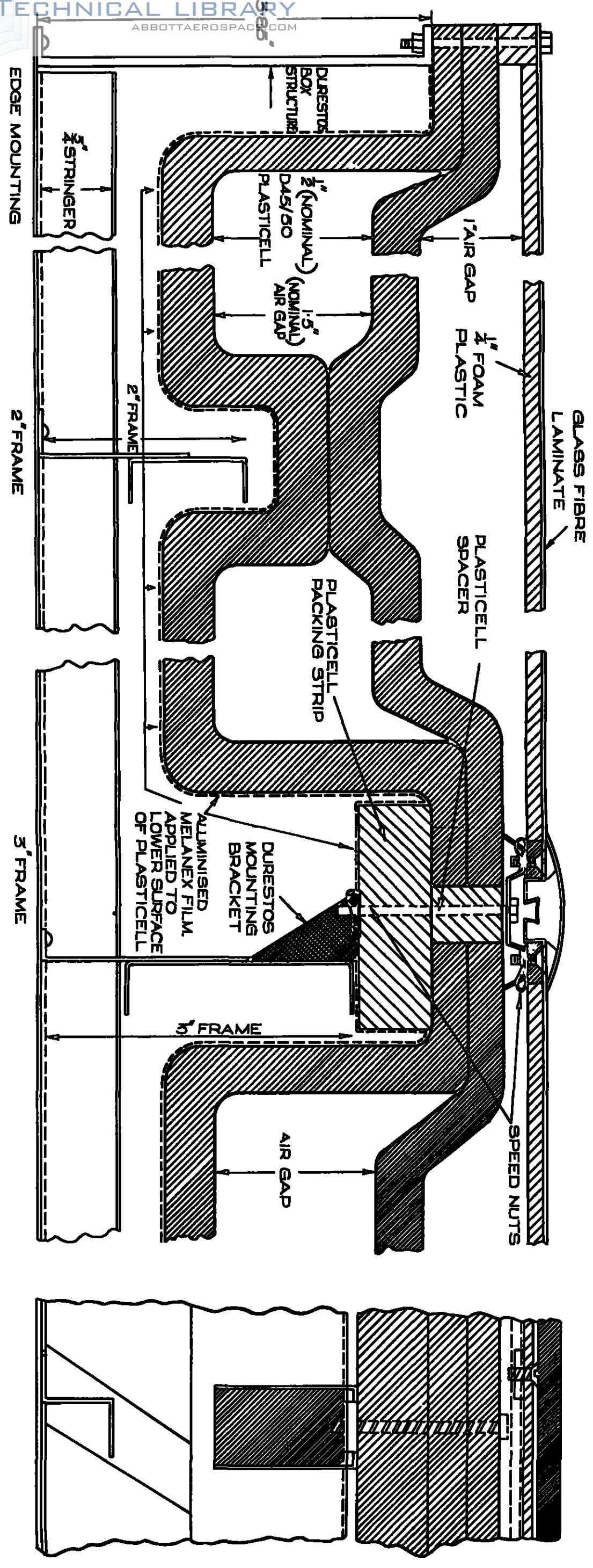
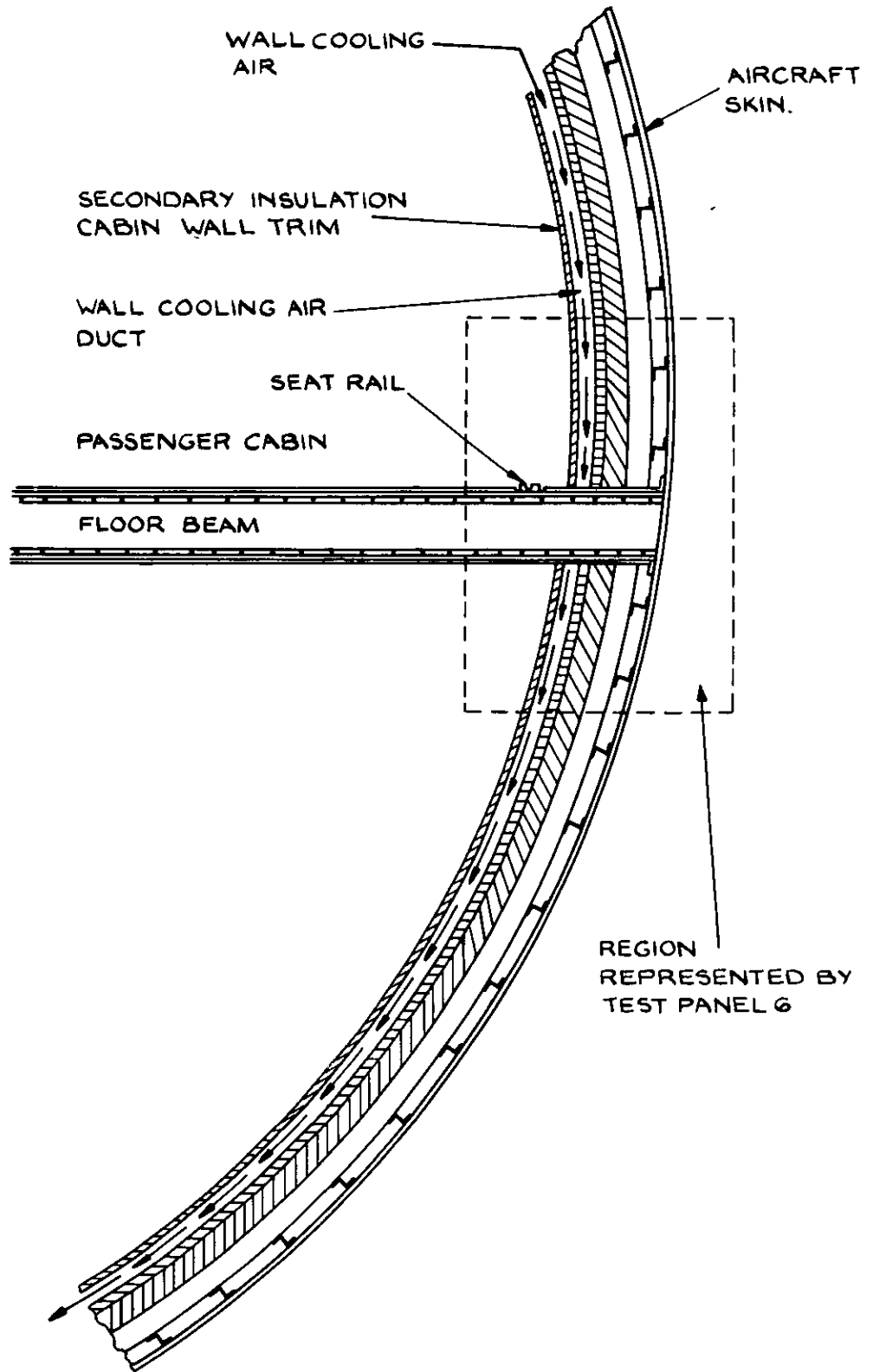


FIG.12. DETAILS OF ATTACHMENT OF INSULATION TO STRUCTURE PRE-FORMED PLASTICELL PANEL. B.198-7.



**FIG.13. DIAGRAM OF FLOOR BEAM ATTACHMENT.
PANEL B198.6**

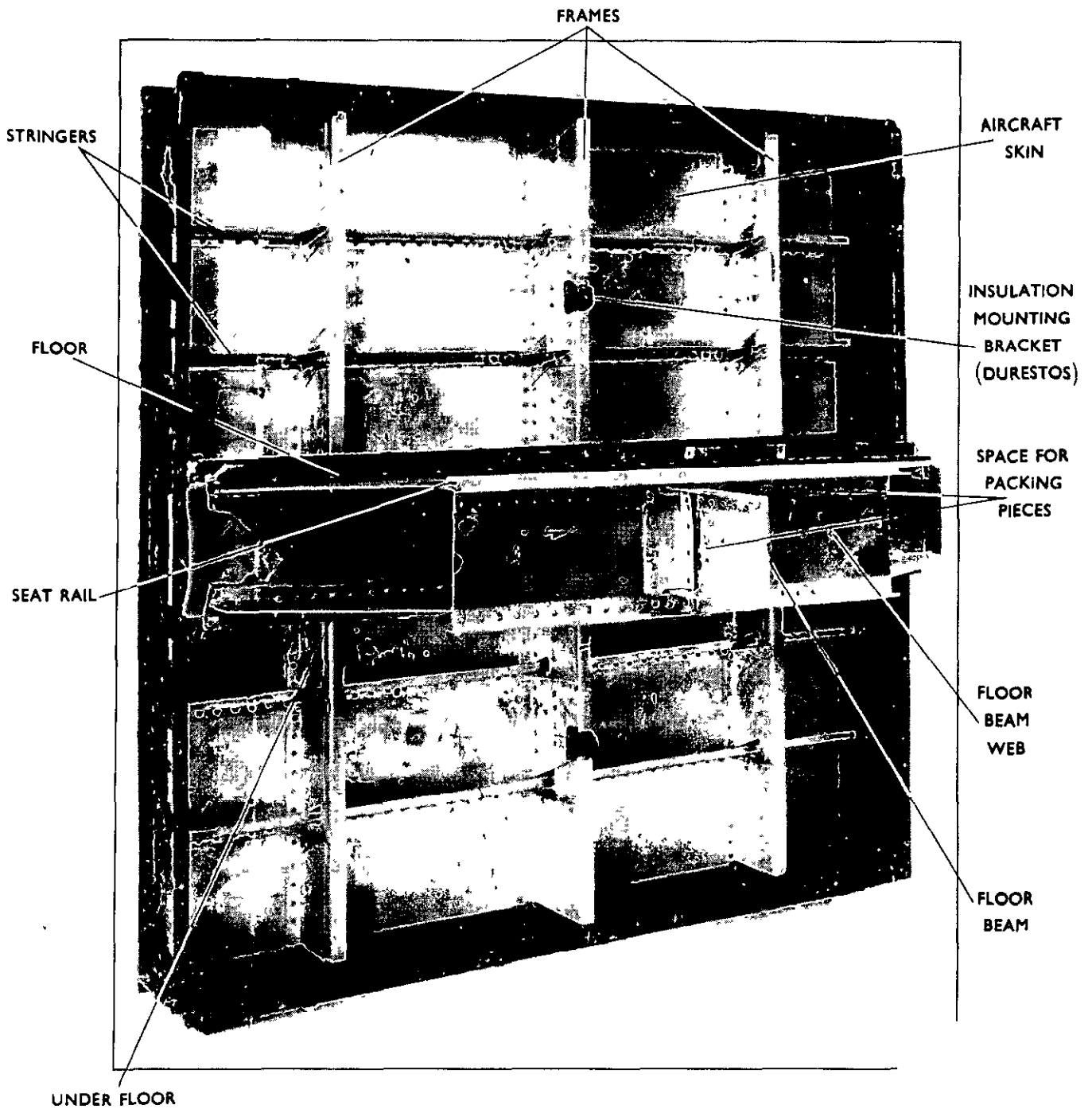


FIG.14 BRISTOL 198 (FLOOR BEAM) PANEL 6

SHOWING STRUCTURAL DETAILS WITH
INSULATION REMOVED

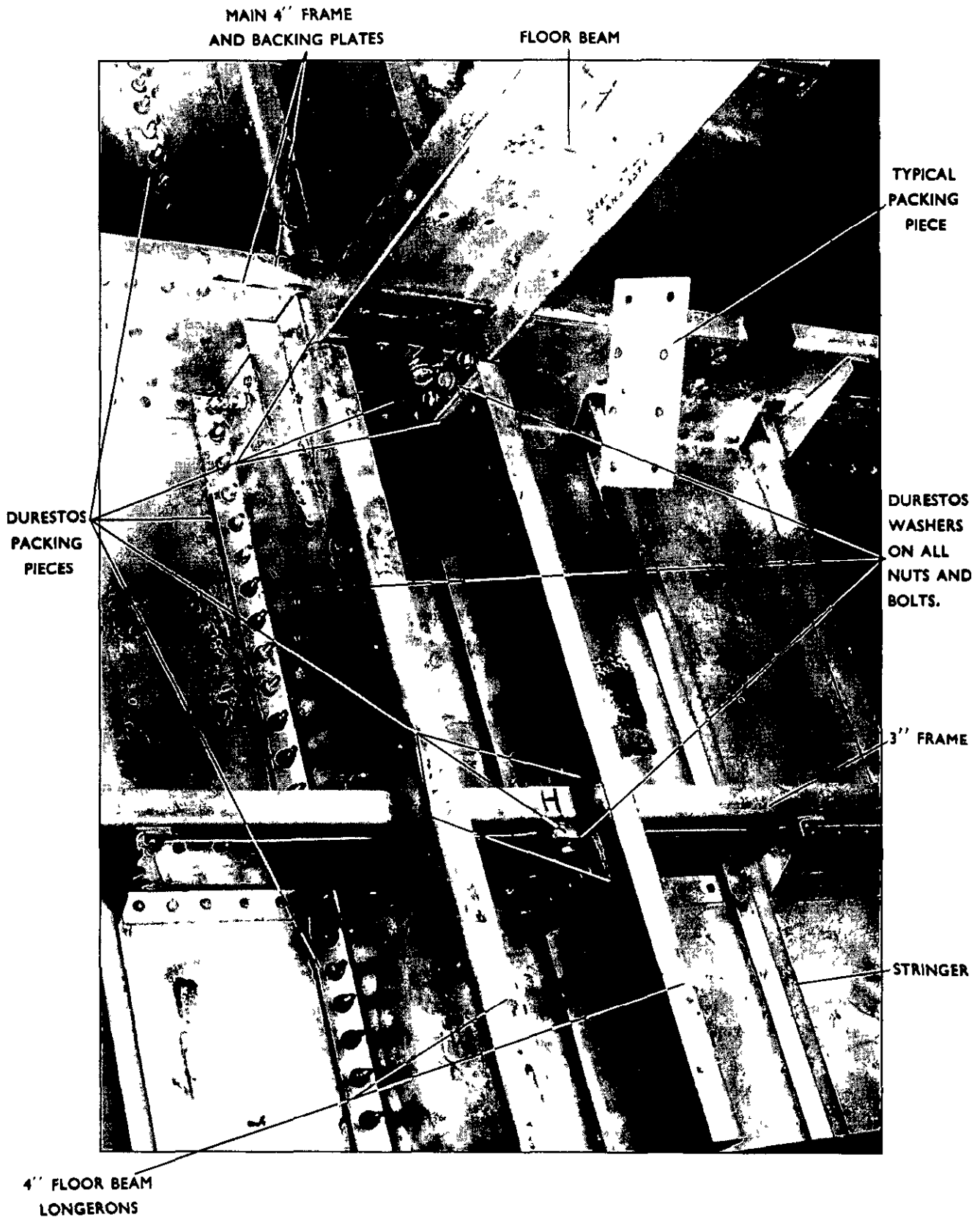


FIG.15 DETAIL OF MODIFIED FLOOR BEAM PANEL

MODIFICATION CONSISTED OF REPLACING METAL PACKING PIECES AND WASHERS WITH SIMILAR ONES MADE OF DURESTOS

FIGURE SHOWS SIMPLIFIED LAYOUT
 OF TEST PANEL N°6 AS
 ASSEMBLED FOR TESTING

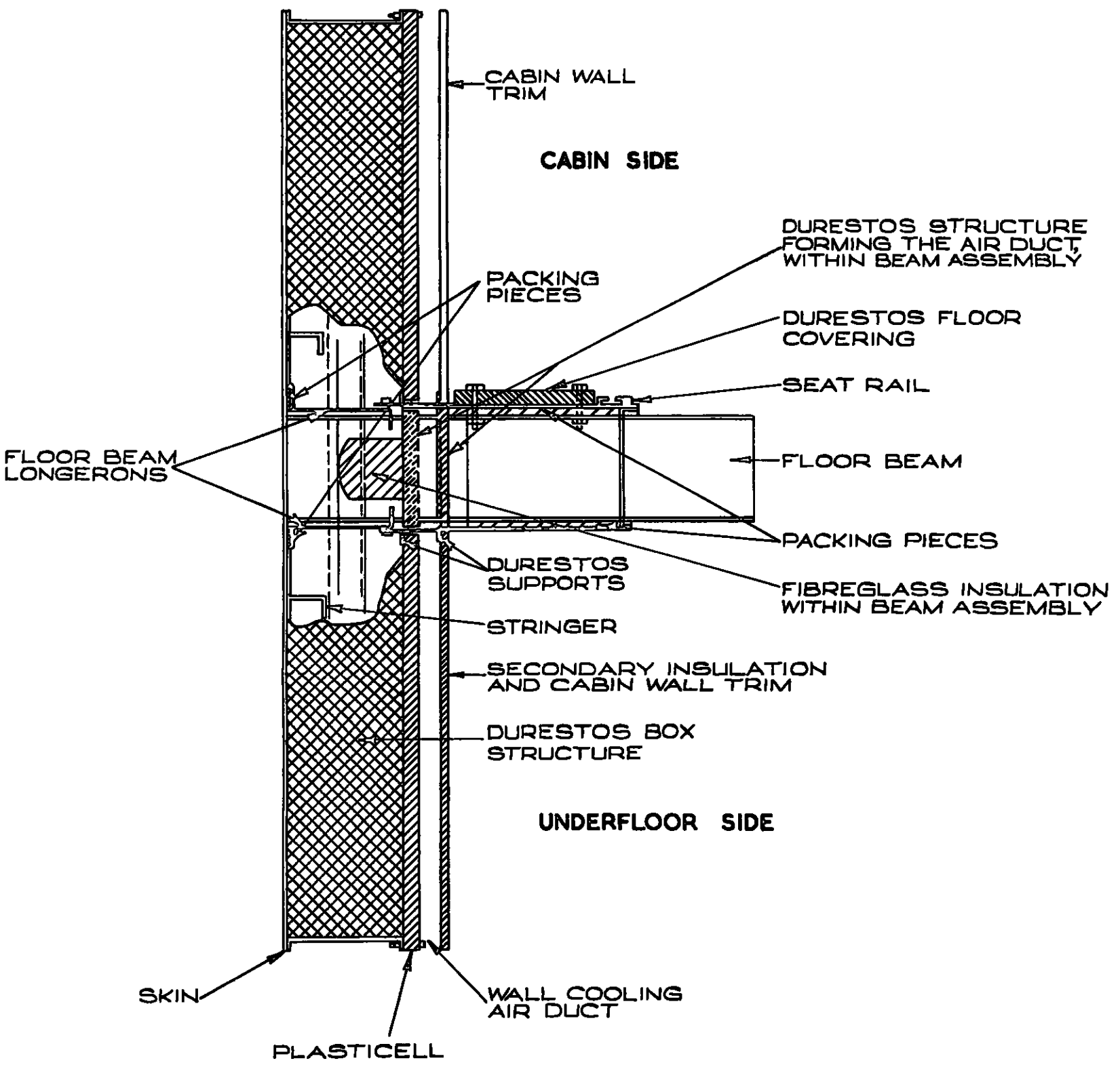
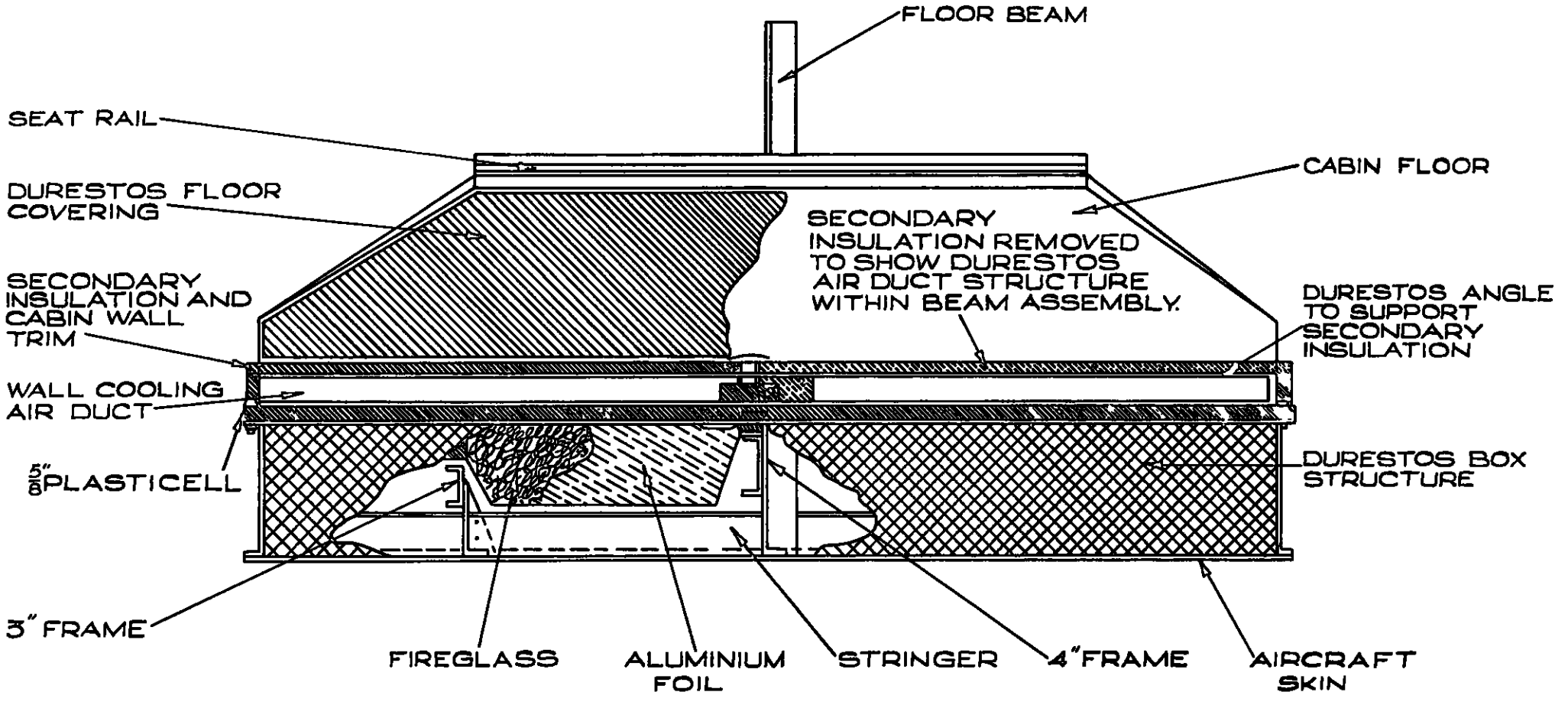
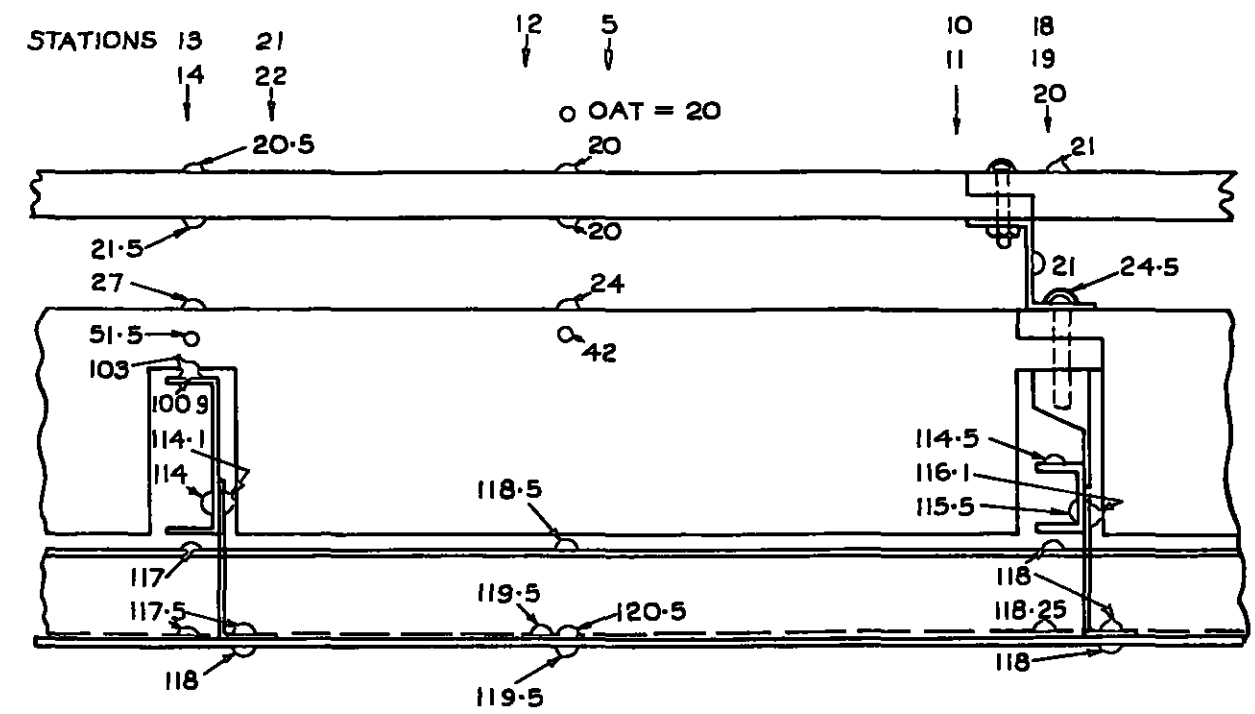
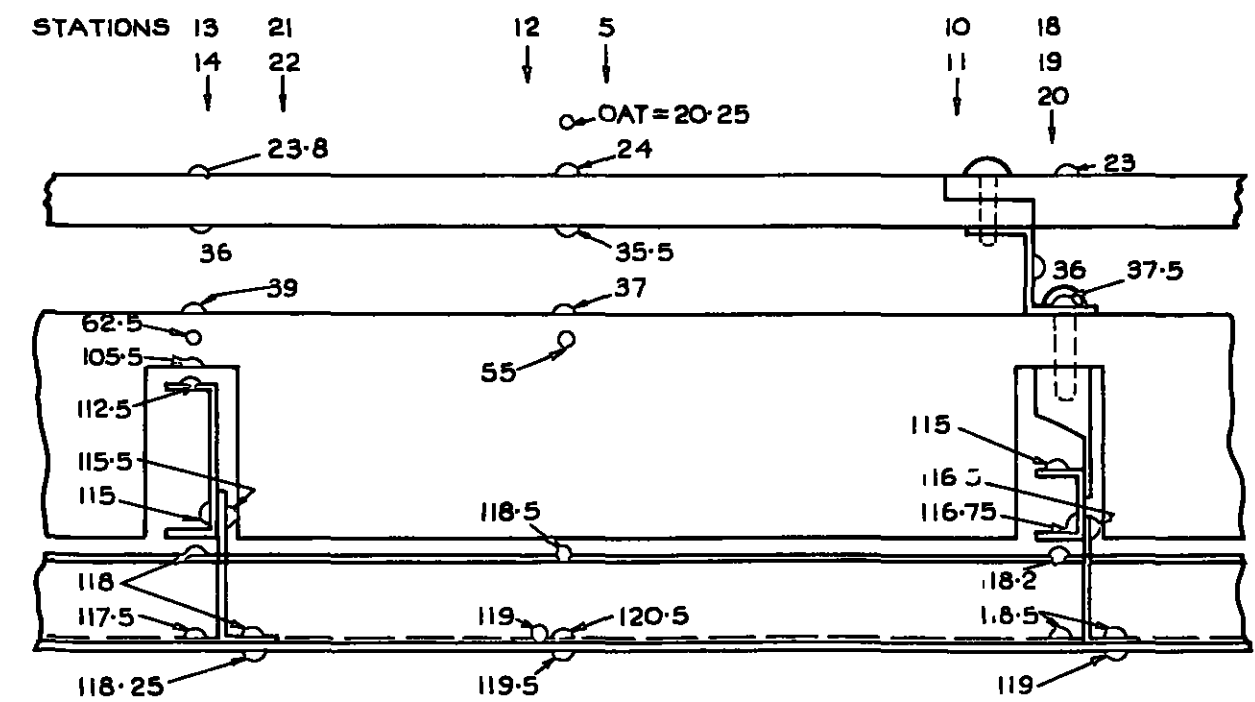


FIG.16. DETAILS OF CONSTRUCTION AND ATTACHMENT PANEL B198-6.



AIR FLOW 6lb/min AT 20°C INLET
 SKIN TEMPERATURE 120°C NOMINAL.



AIR FLOW 6 lb/min AT 33°C INLET
 SKIN TEMPERATURE 120°C NOMINAL.

FIG.17 .TYPICAL TEMPERATURE DISTRIBUTION :
 PANEL B 198-1

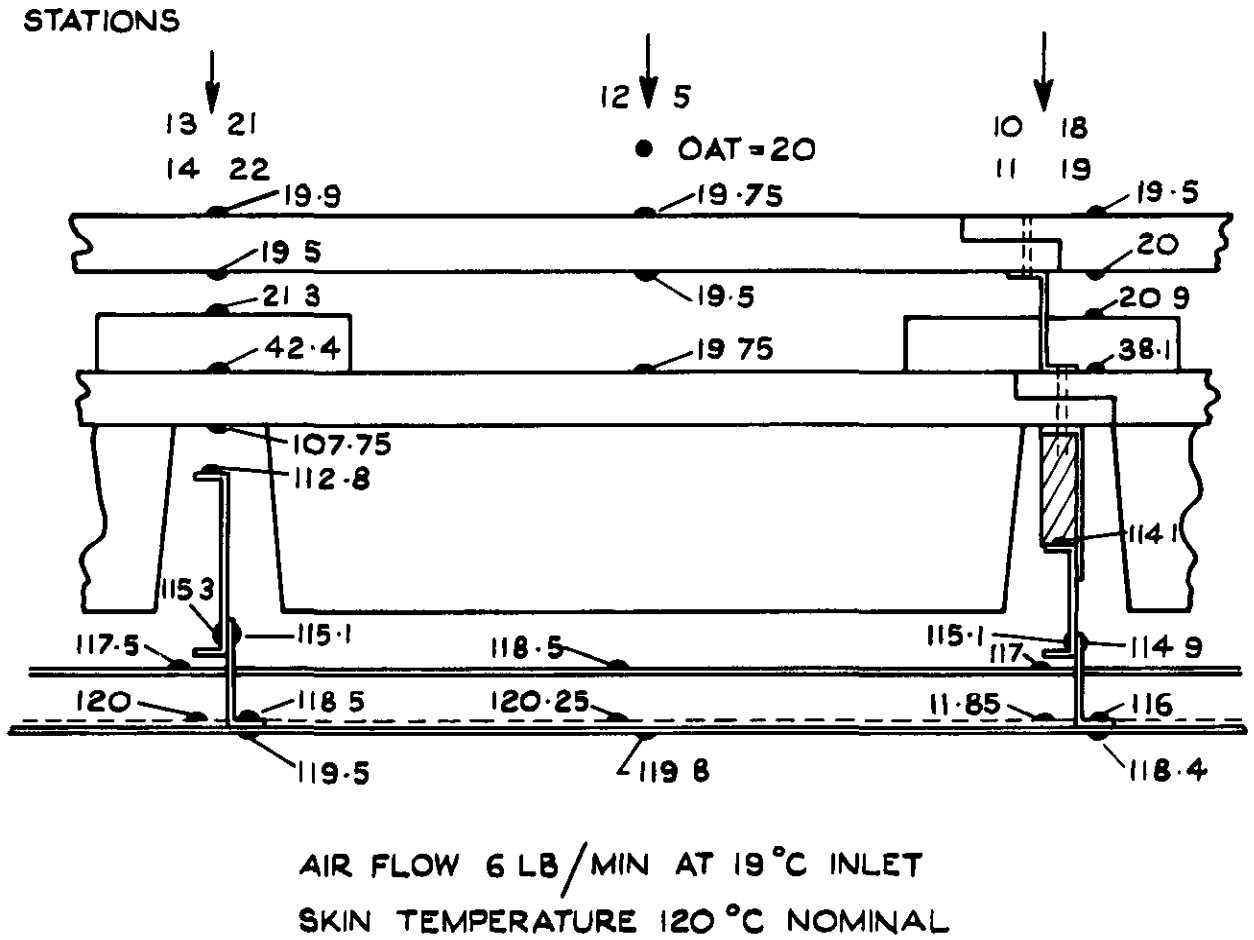
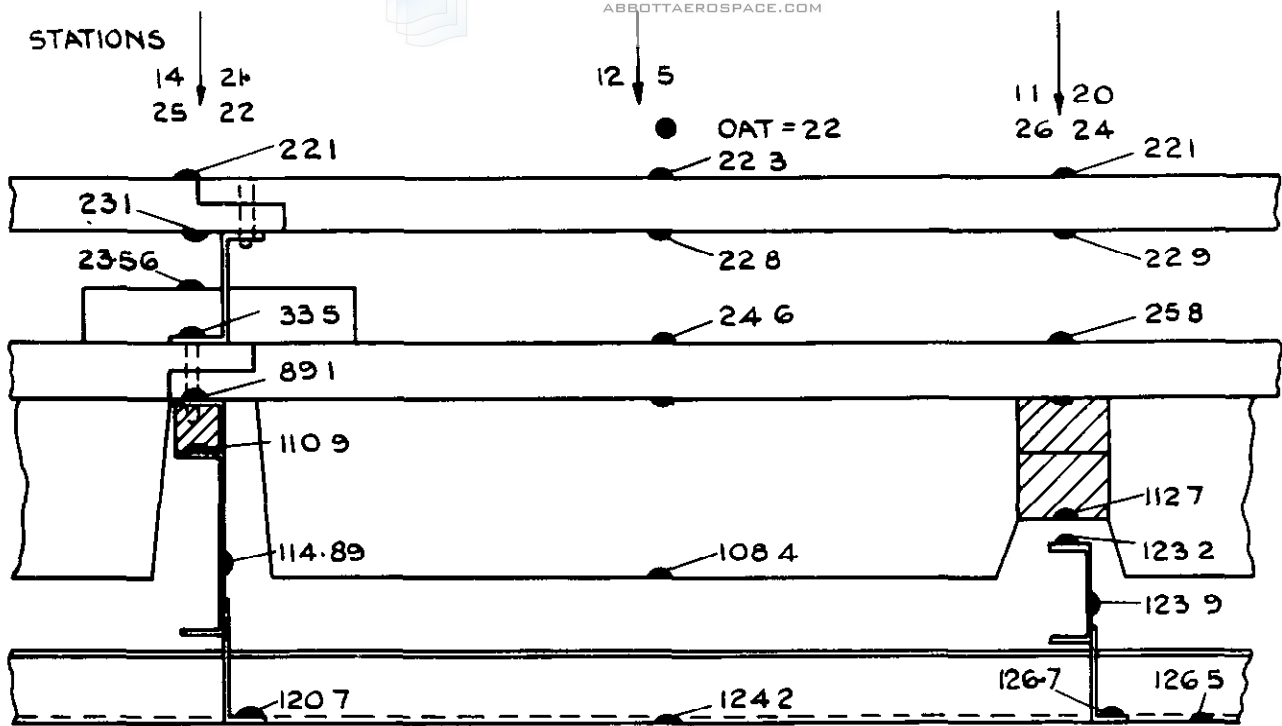
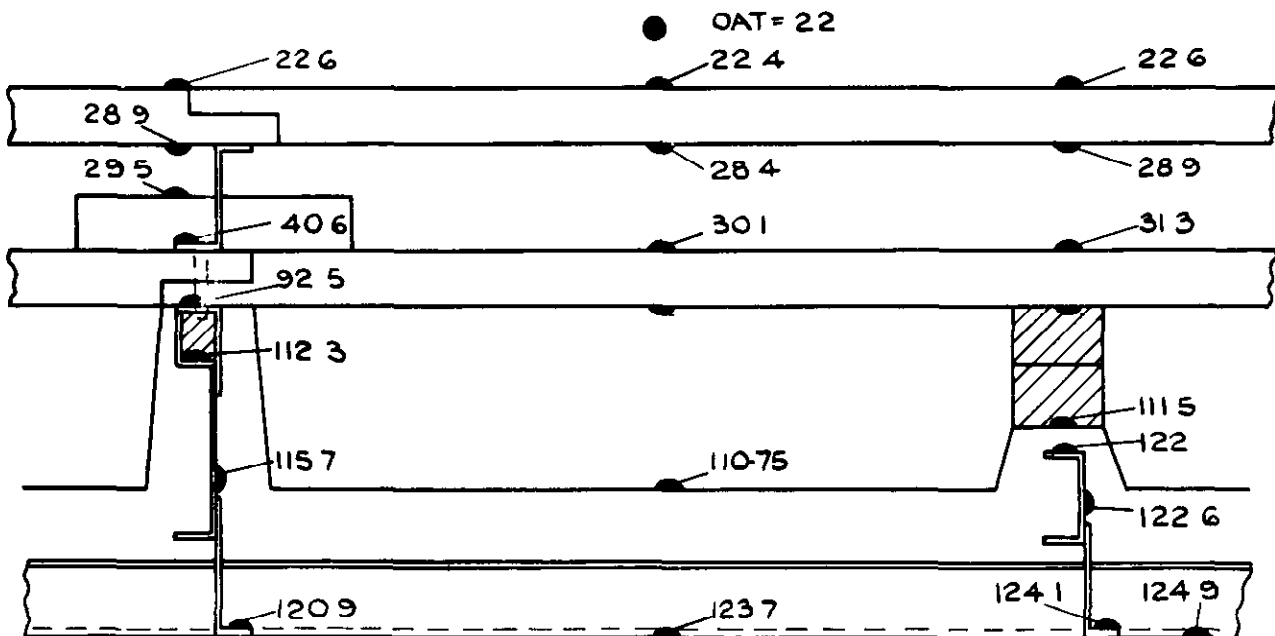


FIG.18. TYPICAL TEMPERATURE DISTRIBUTION
PANEL B192 2 MODIFIED.

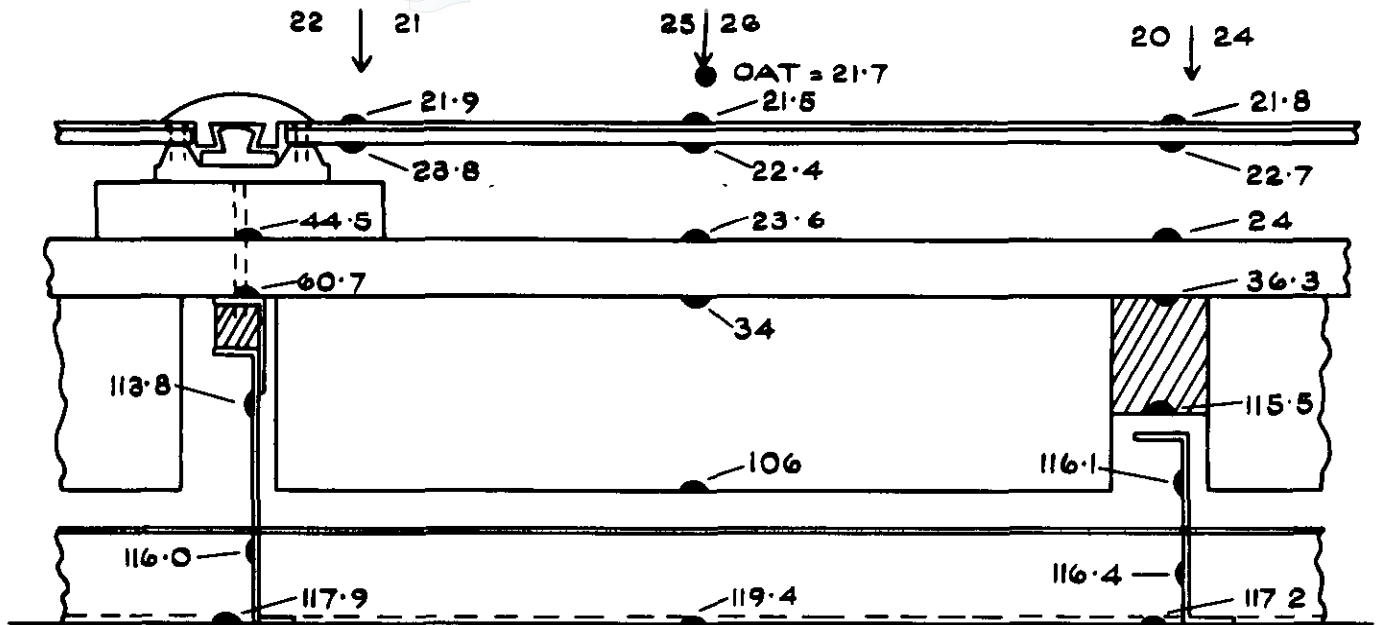


AIR FLOW 6 LB/MIN AT 2219 °C INLET
 SKIN TEMPERATURE 120 °C NOMINAL

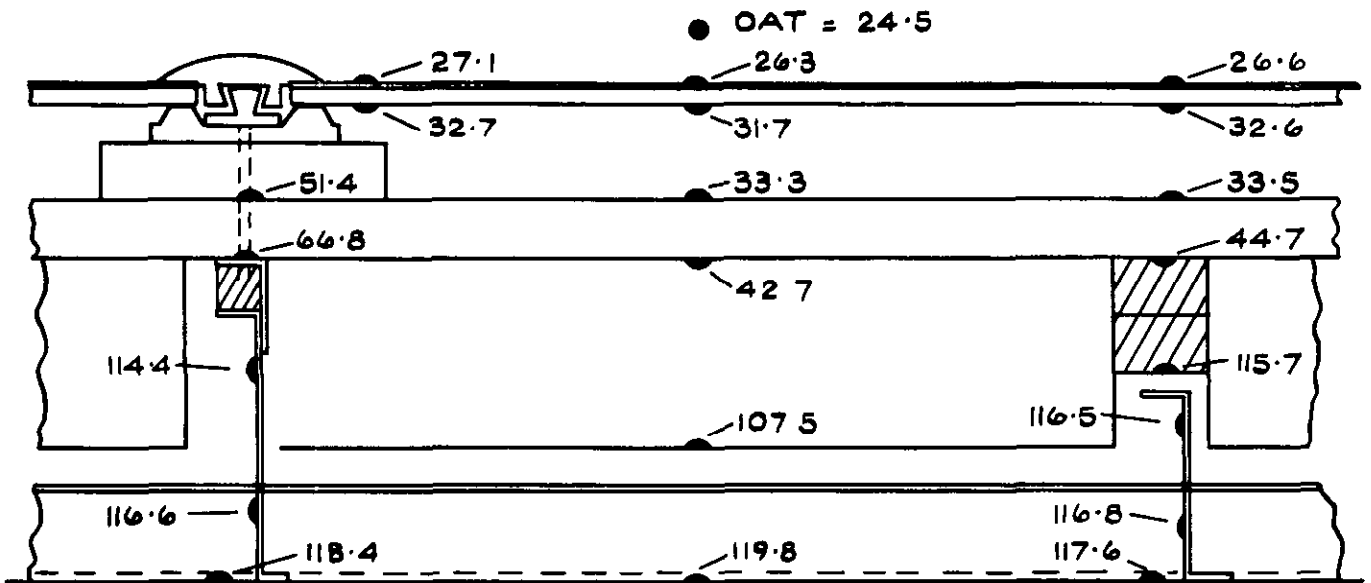


AIR FLOW 6 LB/MIN AT 278 °C INLET
 SKIN TEMPERATURE 120 °C NOMINAL

**FIG.19. TYPICAL TEMPERATURE DISTRIBUTION
 PANEL B198.3.**

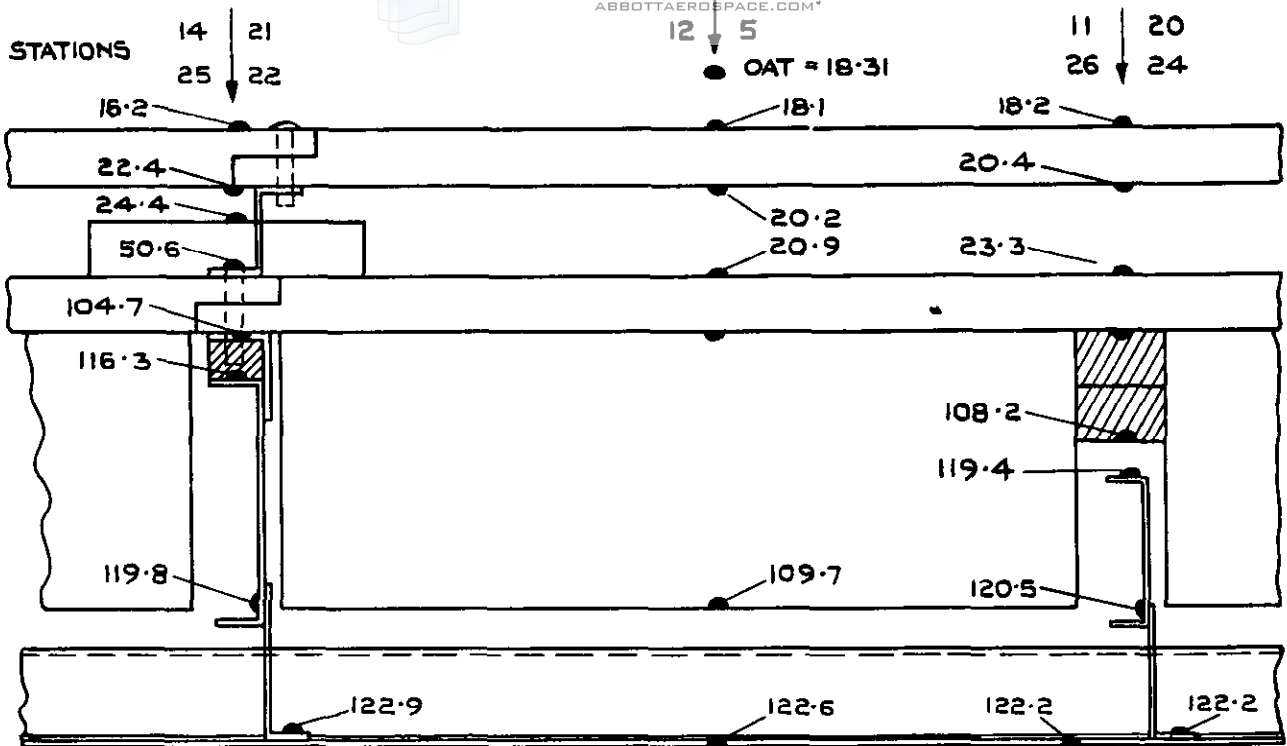


AIR FLOW 6 lb/MIN AT 22°C INLET.
 SKIN TEMPERATURE 120°C NOMINAL.

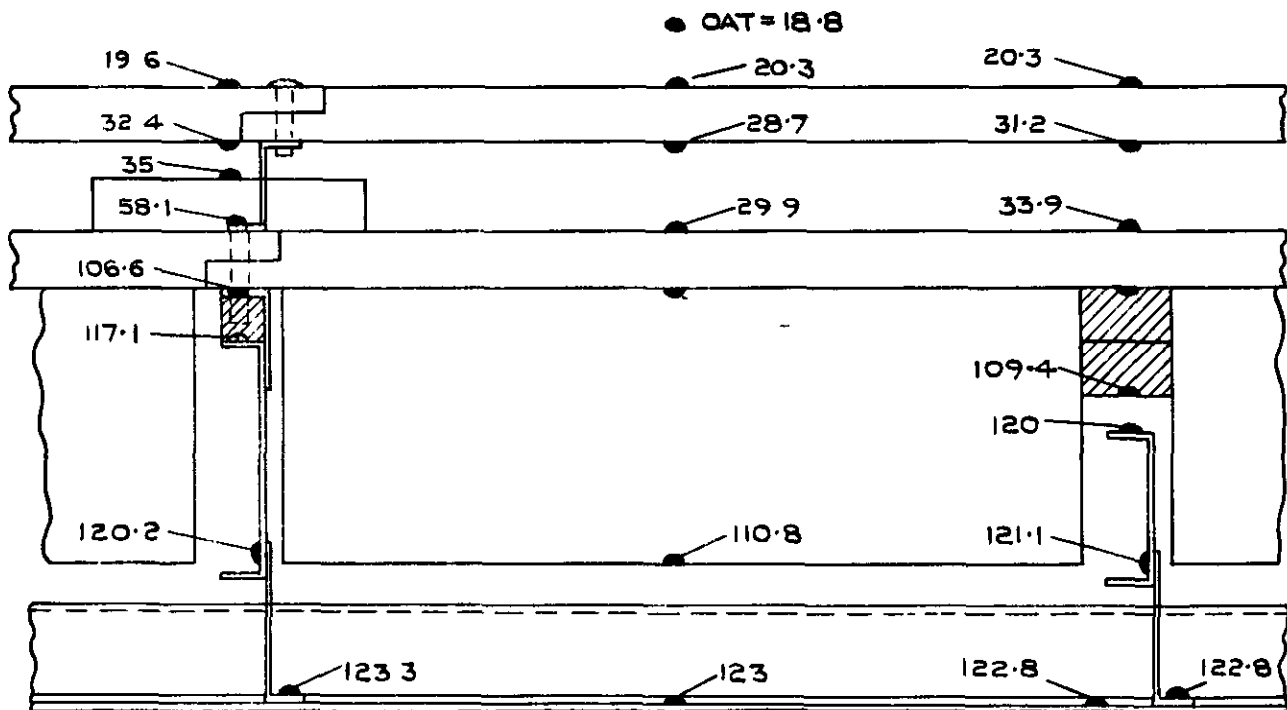


AIR FLOW 6 lb/MIN AT 30.9°C INLET.
 SKIN TEMPERATURE 120°C NOMINAL.

FIG.20. TYPICAL TEMPERATURE DISTRIBUTION. PANEL B198:4.

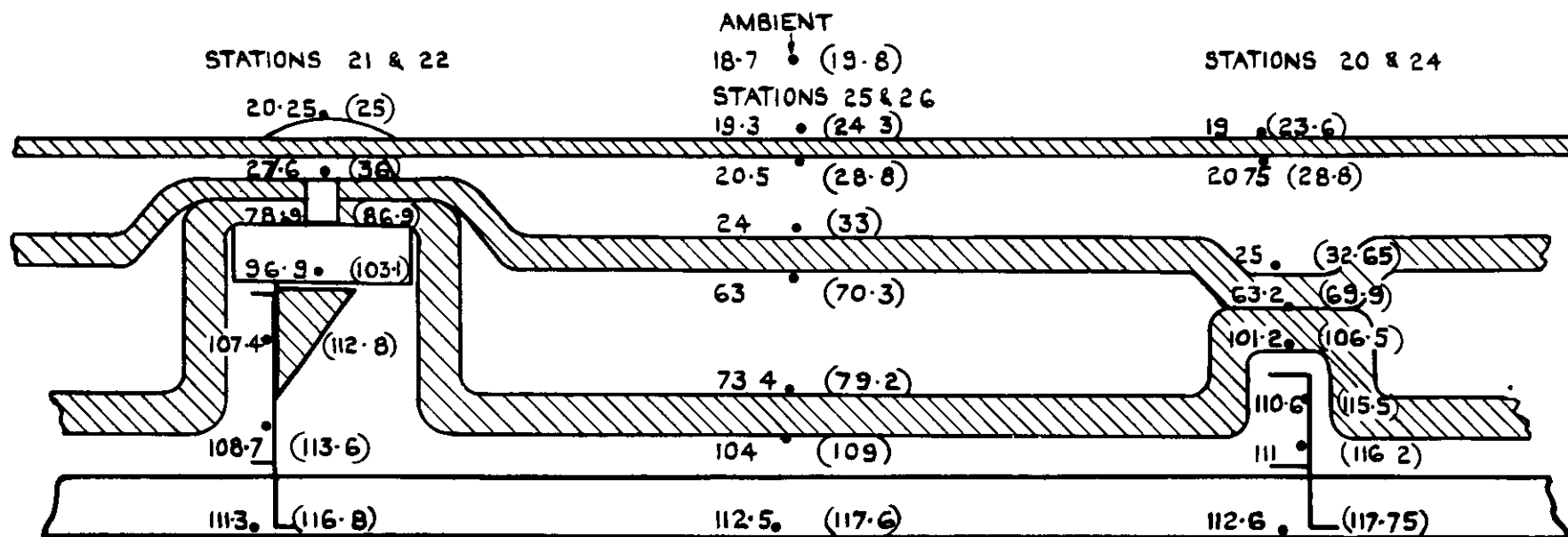


AIR FLOW 6 lb/MIN AT 19.5 °C INLET
 SKIN TEMPERATURE 120 °C NOMINAL



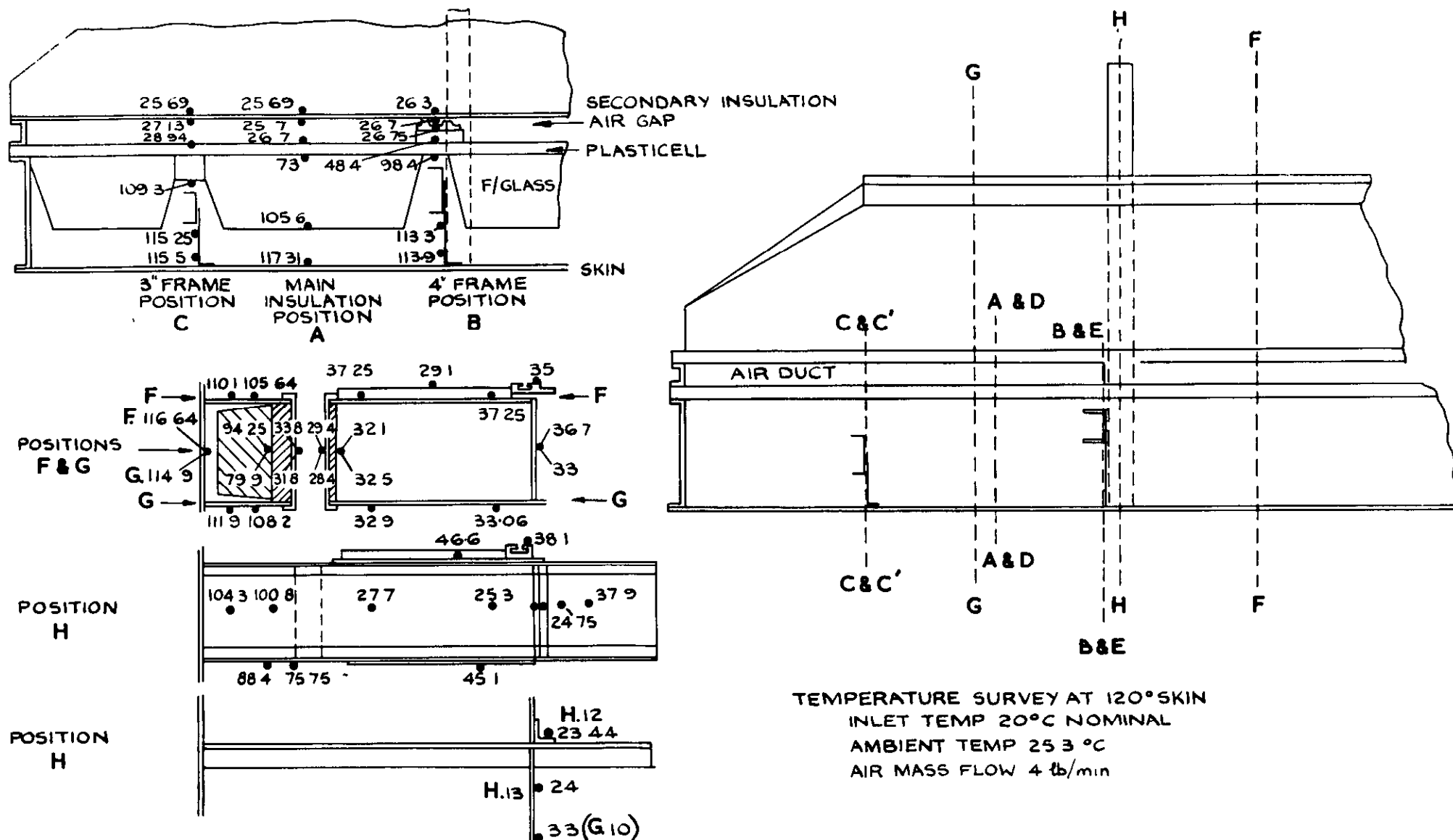
AIR FLOW 6 lb/MIN AT 29.7 °C INLET
 SKIN TEMPERATURE 120 °C NOMINAL

**FIG.21. TYPICAL TEMPERATURE DISTRIBUTION.
 PANEL B.198-5**



MASS FLOW GIB MIN
 MEAN SKIN TEMP. 112.2 AND 117.45
 MEAN AIR INLET TEMP. 18.7 AND 26.9
 THE TEMPERATURE DISTRIBUTION AT THE HIGHER INLET
 TEMPERATURE IS SHOWN BY TEMPERATURES IN BRACKETS.

FIG.22. 9. TYPICAL TEMPERATURE DISTRIBUTION. PANEL B 198-7.



TEMPERATURE SURVEY AT 120° SKIN
 INLET TEMP 20°C NOMINAL
 AMBIENT TEMP 25.3 °C
 AIR MASS FLOW 4 lb/min

FIG.23. TYPICAL TEMPERATURE DISTRIBUTION PANEL B 198/6

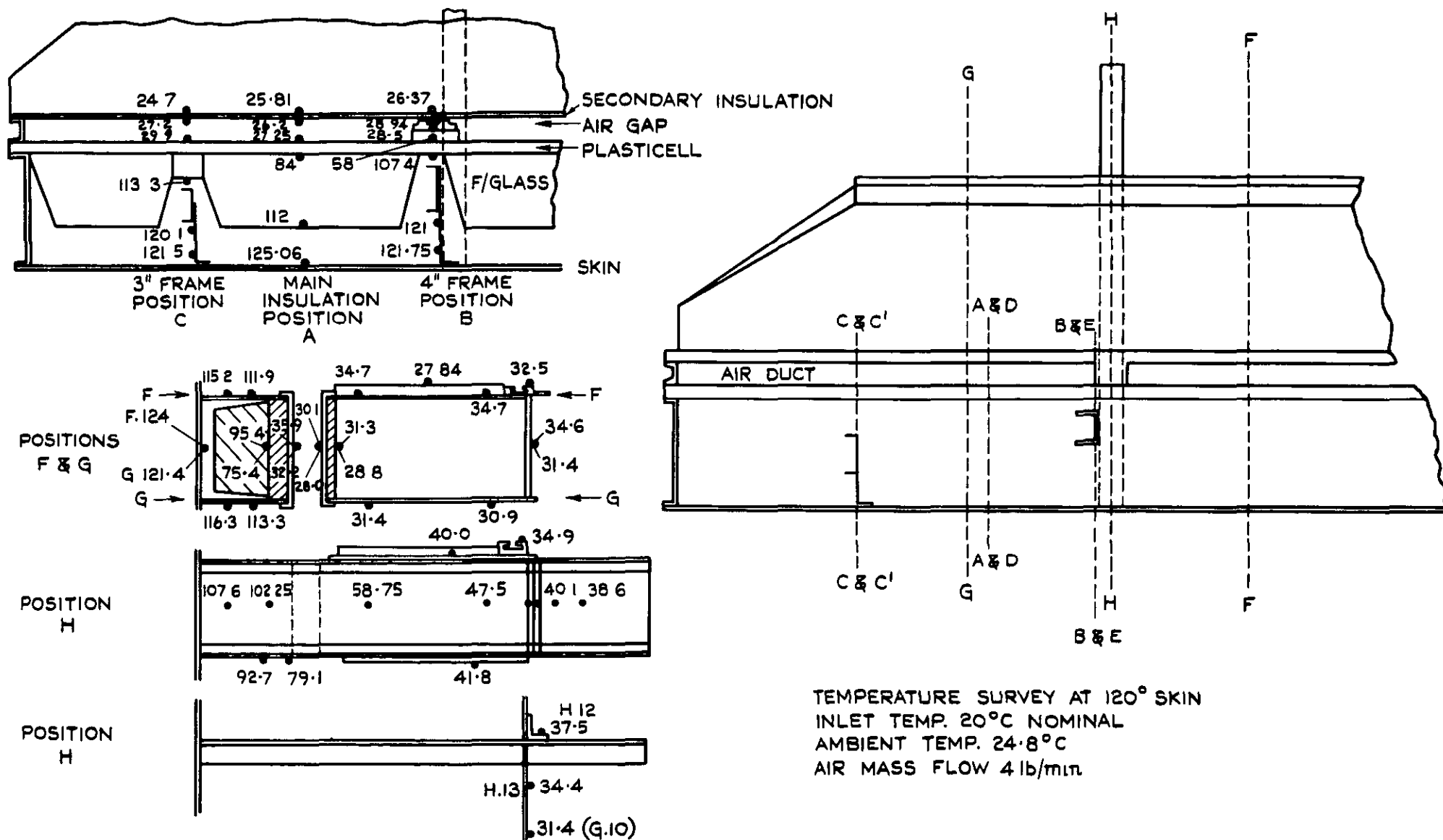


FIG.24. TYPICAL TEMPERATURE DISTRIBUTION. PANEL B198/6. (MODIFIED)

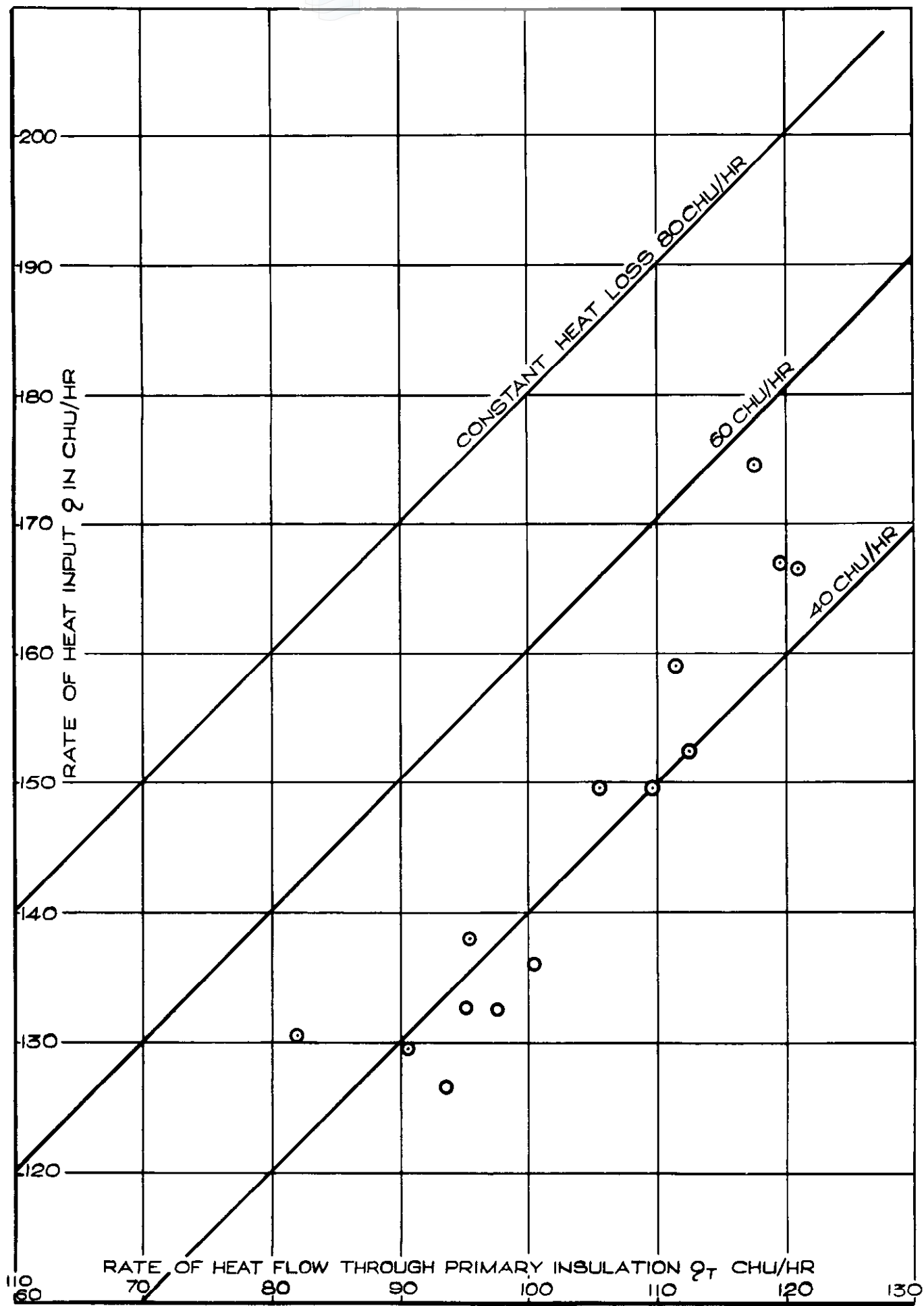


FIG.25 COMPARISON OF HEAT INPUT & CALCULATED HEAT FLOW THROUGH PRIMARY INSULATION PANEL BI98:4

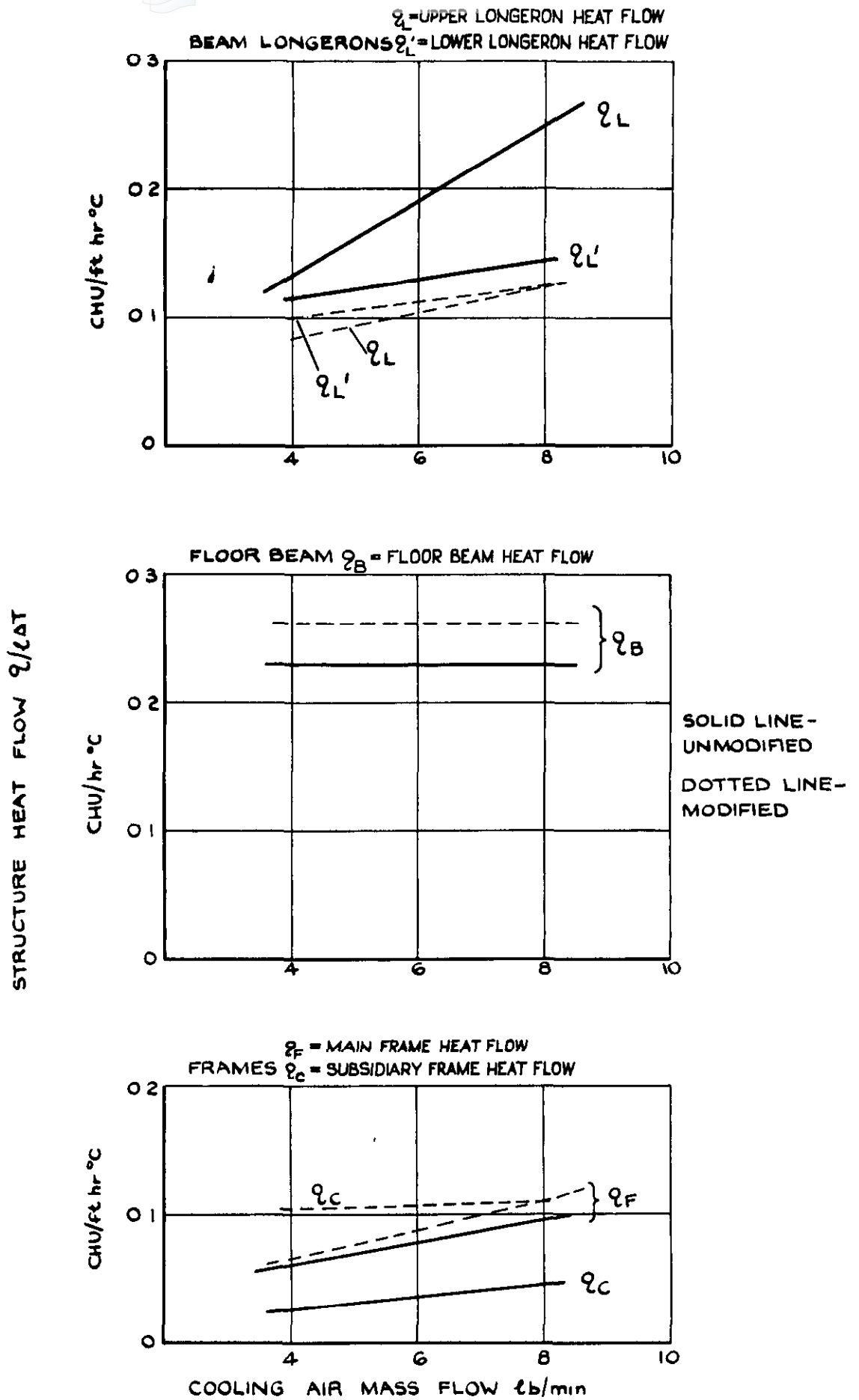


FIG.26. VARIATION OF STRUCTURE HEAT FLOWS WITH COOLING AIR MASS FLOW PANEL B198/6.

A.R.C. C.P. No.910

August 1964

THERMAL CONDUCTANCE TESTS ON CABIN WALL INSULATION
ASSEMBLIES FOR A SUPERSONIC TRANSPORT AIRCRAFT.

McNaughtan, Ian I. and Keene, P.A.

Thermal conductance tests have been made on a number of insulation assemblies for the cabin wall of a supersonic transport aircraft at outer skin temperatures in the range 90-120°C. In all cases the test specimens were assembled onto structure representing the fuselage wall. In addition tests were made on a representative fuselage to floor beam joint. The results of the tests are presented and discussed, and the problems of insulating hot cabin walls are outlined.

536.24 :
629.13.013.1-1/2 :
629.137.1 :
533.6.011-5

A.R.C. C.P. No.910

August 1964

THERMAL CONDUCTANCE TESTS ON CABIN WALL INSULATION
ASSEMBLIES FOR A SUPERSONIC TRANSPORT AIRCRAFT.

McNaughtan, Ian I. and Keene, P.A.

Thermal conductance tests have been made on a number of insulation assemblies for the cabin wall of a supersonic transport aircraft at outer skin temperatures in the range 90-120°C. In all cases the test specimens were assembled onto structure representing the fuselage wall. In addition tests were made on a representative fuselage to floor beam joint. The results of the tests are presented and discussed, and the problems of insulating hot cabin walls are outlined.

536.24 :
629.13.013.1-1/2 :
629.137.1 :
533.6.011-5

A.R.C. C.P. No.910

August 1964

THERMAL CONDUCTANCE TESTS ON CABIN WALL INSULATION
ASSEMBLIES FOR A SUPERSONIC TRANSPORT AIRCRAFT.

McNaughtan, Ian I. and Keene, P.A.

Thermal conductance tests have been made on a number of insulation assemblies for the cabin wall of a supersonic transport aircraft at outer skin temperatures in the range 90-120°C. In all cases the test specimens were assembled onto structure representing the fuselage wall. In addition tests were made on a representative fuselage to floor beam joint. The results of the tests are presented and discussed, and the problems of insulating hot cabin walls are outlined.

536.24 :
629.13.013.1-1/2 :
629.137.1 :
533.6.011-5

C.P. No. 910

© *Crown Copyright 1967*

Published by
HER MAJESTY'S STATIONERY OFFICE

To be purchased from
49 High Holborn, London w c 1
423 Oxford Street, London w 1
13A Castle Street, Edinburgh 2
109 St. Mary Street, Cardiff
Brazennose Street, Manchester 2
50 Fairfax Street, Bristol 1
35 Smallbrook, Ringway, Birmingham 5
80 Chichester Street, Belfast 1
or through any bookseller

C.P. No. 910

S O CODE No. 23-9017-10